Pepper Arginine Decarboxylase Is Required for Polyamine and γ-Aminobutyric Acid Signaling in Cell Death and Defense Response[1][C][W][OPEN]

Nak Hyun Kim, Beom Seok Kim, and Byung Kook Hwang*

College of Life Sciences and Biotechnology, Korea University, Seoul 136–713, Republic of Korea

The *Xanthomonas campestris* pv *vesicatoria* (*Xcv*) effector AvrBsT induces a hypersensitive cell death in pepper (*Capsicum annuum*). However, the molecular mechanisms underlying AvrBsT-triggered cell death are not fully understood. Here, we identified pepper arginine decarboxylase (CaADC1) as an AvrBsT-interacting protein, which is early and strongly induced in incompatible pepper-*Xcv* interactions. Bimolecular fluorescence complementation and coimmunoprecipitation assays showed that the CaADC1-AvrBsT complex was localized to the cytoplasm. Transient coexpression of *CaADC1* with *avrBsT* in *Nicotiana benthamiana* leaves specifically enhanced AvrBsT-triggered cell death, accompanied by an accumulation of polyamines, nitric oxide (NO), and hydrogen peroxide (H_2O_2) bursts. Among the polyamines, spermine application strongly induced NO and H_2O_2 bursts, ultimately leading to cell death. *CaADC1* silencing in pepper leaves significantly compromised NO and H_2O_2 accumulation and cell death induction, leading to the enhanced avirulent *Xcv* growth during infection. The levels of salicylic acid, polyamines, and γ-aminobutyric acid (GABA), and the expression of defense response genes during avirulent *Xcv* infection, were distinctly lower in *CaADC1*-silenced plants than those in the empty vector control plants. GABA application significantly inhibited avirulent *Xcv* growth in *CaADC1*-silenced leaves and the empty vector control plants. Together, these results suggest that *CaADC1* may act as a key defense and cell death regulator via mediation of polyamine and GABA metabolism.

The activation of plant defense signaling induces massive transcriptional reprogramming, leading to the accumulation of pathogenesis-related (PR) proteins, reactive oxygen species (ROS), phytoalexins, and various defense-related metabolites (Asai et al., 2002; Garcia-Brugger et al., 2006; Berger et al., 2007). Polyamines (PAs), including putrescine, spermidine, and spermine, are positively charged small metabolites that are implicated in plant disease resistance and other physiological processes such as cell proliferation, differentiation, morphogenesis, flowering, senescence, seed dormancy, and germination (Walden et al., 1997; Martin-Tanguy, 2001; Walters, 2003a; Deeb et al., 2010). PAs have been shown to confer protection against abiotic stresses such as mineral nutrient deficiency, salt, drought, cold, and oxidative stress (Bouchereau et al., 1999; Kasinathan and Wingler, 2004).

In plants, PAs are synthesized from the amino acids Orn or Arg via decarboxylation (Walters, 2003a). Decarboxylation of Orn or Arg is catalyzed by ornithine decarboxylase (ODC; EC 4.1.1.17) or arginine decarboxylase (ADC; EC 4.1.1.19) and yields putrescine or agmatine, respectively (Walters, 2003b). Agmatine is hydrolyzed by agmatine deiminase (EC 3.5.3.12) to *N*-carbamoylputrescine, which in turn is hydrolyzed by *N*-carbamoylputrescine amidohydrolase (EC 3.5.1.53) to putrescine (Janowitz et al., 2003; Piotrowski et al., 2003). Spermidine is synthesized from putrescine via the addition of aminopropyl groups to putrescine by spermidine synthase (EC 2.5.1.16; Bagni and Tassoni, 2001; Walters, 2003b). Spermine is synthesized via the addition of aminopropyl groups to spermidine by spermine synthase (EC 2.5.1.22; Bagni and Tassoni, 2001; Walters, 2003b).

ODC and ADC act as rate-limiting factors in PA biosynthesis and play pivotal roles in PA metabolism (Bagni and Tassoni, 2001). Perturbation of endogenous PA levels by ODC and ADC affects various physiological processes in plants (Capell et al., 2004; Kasinathan and Wingler, 2004; Alcázar et al., 2005). Transgenic Arabidopsis overexpressing *ADC* displayed dwarf stature and exhibited delayed flowering (Alcázar et al., 2005). Transgenic rice (*Oryza sativa*) overexpressing *ADC* had higher tolerance to drought stress (Capell et al., 2004). Transgenic tobacco (*Nicotiana tabacum*) with increased ODC activity was more tolerant to salt stress, whereas Arabidopsis (*Arabidopsis thaliana*) mutants with reduced ADC activity were less tolerant to salt stress

[1] This work was supported by the Next Generation BioGreen21 Program, Rural Development Administration, Republic of Korea (grant no. PJ008027).

* Corresponding author; e-mail bkhwang@korea.ac.kr.

The author responsible for distribution of materials integral to the findings presented in this article in accordance with the policy described in the Instructions for Authors (www.plantphysiol.org) is: Byung Kook Hwang (bkhwang@korea.ac.kr).

[C] Some figures in this article are displayed in color online but in black and white in the print edition.

[W] The online version of this article contains Web-only data.

[OPEN] Articles can be viewed online without a subscription.

www.plantphysiol.org/cgi/doi/10.1104/pp.113.217372

(Kumria and Rajam, 2002; Kasinathan and Wingler, 2004).

The disease resistance response and protection against abiotic stresses conferred by PAs are intimately related to a ROS burst (Takahashi et al., 2004; Moschou et al., 2008). ROS directly inhibit pathogen growth, stimulate cross-linking of the cell wall, and mediate signal transduction for the expression of defense- and stress-responsive genes (Lamb and Dixon, 1997; Skopelitis et al., 2006). The oxidation of PAs in the apoplast, which is a major source of the ROS burst, is mediated by NADPH oxidases or peroxidases in the plasma membrane or cell wall, respectively (Takahashi et al., 2004). Spermidine is oxidized by polyamine oxidase (EC 1.5.3.3) to diaminopropane, pyrroline, and hydrogen peroxide (H_2O_2). Polyamine oxidase also oxidizes spermine to diaminopropane, aminopropylpyrroline, and H_2O_2. Putrescine is converted by diamine oxidase (EC 1.4.3.22) to pyrroline, ammonia, and H_2O_2 (Bagni and Tassoni, 2001).

Pyrroline can be further processed to form γ-aminobutyric acid (GABA), a nonprotein amino acid that is best known as an inhibitory neurotransmitter in the mammalian central nervous system (Bhat et al., 2010) and as an intracellular signaling molecule in plant development and stress responses (Roberts, 2007). GABA is involved in nitrogen metabolism, protection against oxidative stress, osmoregulation, and defense against herbivorous pests (Bouché and Fromm, 2004). Arabidopsis *ssadh* mutants that are defective in GABA catabolism were hypersensitive to photodamage and heat, leading to cell death and the concomitant accumulation of high levels of H_2O_2 (Bouché et al., 2003). Plant GABA was proposed to mediate quorum-sensing in *Agrobacterium tumefaciens*, thereby affecting its virulence on plants (Chevrot et al., 2006). Plant-produced GABA is imported into *A. tumefaciens*, where it induces the lactonase AttM (BlcC), which degrades the quorum-sensing signal and attenuates bacterial virulence. Plant L-proline was demonstrated to antagonize GABA-induced quenching of quorum-sensing in *A. tumefaciens* (Haudecoeur et al., 2009). Both GABA and proline are taken up by a specific ABC transporter in concert with the periplasmic binding protein Atu2422. More recently, it has been reported that a bacterial small RNA controls uptake of a plant-generated signaling molecule GABA into bacteria (Wilms et al., 2011). The periplasmic binding protein, Atu2422, which is essential for the transportation of GABA into *A. tumefaciens*, is negatively regulated by a conserved small RNA AbcR1. GABA transaminase-deficient *Pseudomonas syringae* mutants showed significantly reduced virulence, suggesting that GABA has multiple effects on pathogen-plant interactions with increased disease resistance (Park et al., 2010).

The relationship of ROS to plant cell death and/or defense signaling has been extensively documented (Torres et al., 2006; Van Breusegem and Dat, 2006). The ROS burst and plant cell death are hallmarks of the hypersensitive response (HR) that results from pathogen recognition (Lamb and Dixon, 1997). The HR is characterized by rapid local cell death at the site of pathogen invasion, which often leads to systemic and broad-spectrum disease resistance termed systemic acquired resistance (Durrant and Dong, 2004). *Xanthomonas campestris* pv *vesicatoria* (*Xcv*) strain Bv5-4a harbors the type III effector protein AvrBsT and triggers hypersensitive cell death in pepper (*Capsicum annuum*) plants on infection (Kim et al., 2010). Expression of *avrBsT* in the *Xcv* strain Ds1 rendered the strain avirulent to pepper plants. Infection with *Xcv* Ds1 (*avrBsT*) expressing *avrBsT* triggered cell death in pepper leaves. The hypersensitive cell death response elicited by AvrBsT is reminiscent of the resistance (*R*) gene-mediated defense system in plants (Eitas and Dangl, 2010; Kim et al., 2010). However, the precise molecular mechanisms underlying AvrBsT recognition and cell death initiation remain to be elucidated. Identifying host proteins that interact with AvrBsT will provide a basis for understanding cell death and molecular defense mechanisms.

In this study, we identified pepper ADC (CaADC1) as an AvrBsT-interacting protein by using yeast two-hybrid screening. The interaction of CaADC1 and AvrBsT was visualized in the cytoplasm. Transient coexpression of CaADC1 and AvrBsT in *Nicotiana benthamiana* significantly enhanced AvrBsT-triggered cell death. *CaADC1* expression induced the accumulation of PAs and triggered NO and H_2O_2 bursts in *N. benthamiana* leaves. In pepper, the expression of *CaADC1* was rapidly and strongly induced by inoculation with *Xcv* Ds1 (*avrBsT*). *CaADC1*-silenced pepper plants that were susceptible to avirulent *Xcv* Ds1 (*avrBsT*) infection did not exhibit increases in NO and H_2O_2 levels or cell death responses. The level of salicylic acid (SA) and the expression of defense response genes also were compromised by *CaADC1* silencing. PA levels were greatly reduced in *CaADC1*-silenced pepper leaves during *Xcv* infection. Notably, spermine levels were only compromised during avirulent *Xcv* Ds1 (*avrBsT*) infection. *Xcv* Ds1 (*avrBsT*) infection did not induce GABA accumulation in *CaADC1*-silenced plants, which suggests that the nonprotein amino acid GABA may contribute to *R* gene-mediated resistance against avirulent *Xcv* infection. Taken together, the results of this study suggest that *CaADC1* expression induces increased PA and GABA levels and triggers NO and H_2O_2 bursts, ultimately leading to plant defense and cell death responses.

RESULTS

Identification of CaADC1 as an AvrBsT-Interacting Protein

AvrBsT is a type III effector protein of *Xcv* that elicits the hypersensitive cell death in pepper and *N. benthamiana* leaves (Orth et al., 2000; Escolar et al., 2001). To identify the molecular components that interact with AvrBsT, we used the yeast two-hybrid system (Fig. 1). AvrBsT was used as bait, and then we screened a pepper complementary DNA (cDNA) prey library that was generated from leaves undergoing the hypersensitive cell death. Approximately 35,000 transformants were

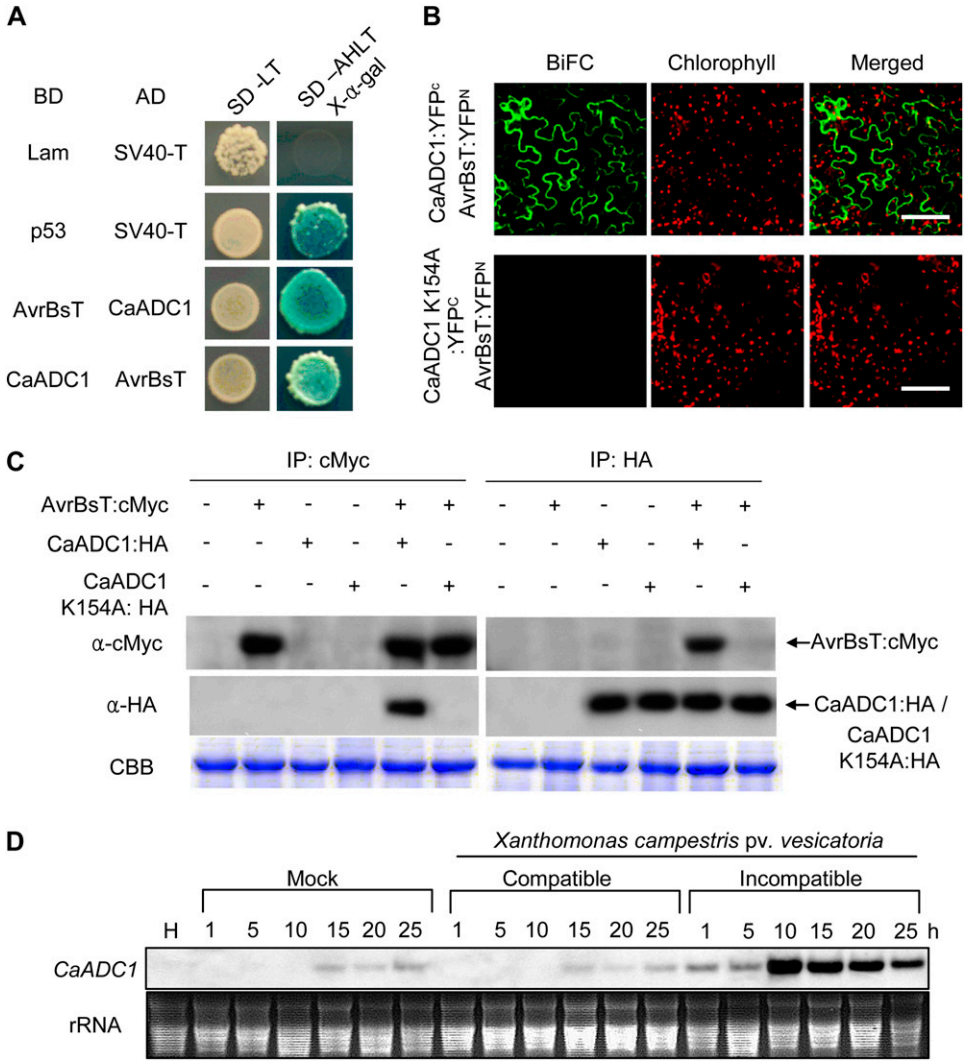

Figure 1. Interactions of CaADC1 with AvrBsT and CaADC1 expression patterns. A, Yeast two-hybrid assay of CaADC1 and AvrBsT. CaADC1 and AvrBsT fused with activation (AD) or binding (BD) domains of GAL4 were cointroduced into *Saccharomyces cerevisiae* strain AH109, and reporter gene activation was monitored on synthetic dropout media (Ala [SD-A], His [SD-H], Leu [SD-L], or Trp [SD-T]) containing X-α-galactose. Lam and p53 combinations with SV40-T were used as negative and positive controls, respectively. B, BiFC analyses of the CaADC1 and AvrBsT interaction in planta. *N. benthamiana* leaves were infiltrated with a mixture of *A. tumefaciens* carrying 35S:*CaADC1*::*YFP*^{C}, 35S:*CaADC1 K154A*:*YFP*^{C}, and 35S:*avrBsT*::*YFP*^{N}. YFP fluorescence in epidermal cells was observed by a confocal microscope at 40 h after agroinfiltration. CBB, Coomassie Brilliant Blue. Bars = 50 μm. C, Coimmunoprecipitation (IP) and immunoblotting of AvrBsT:cMyc and CaADC1:HA or CaADC1 K154A:HA proteins coexpressed in *N. benthamiana* leaves. D, RNA gel-blot analyses of *CaADC1* expression in pepper leaves infected with virulent (Ds1) or avirulent (Bv5-4a) *Xcv*. The mock control was treated with 10 mM $MgCl_2$. H, Healthy leaves. [See online article for color version of this figure.]

screened, and 12 positive clones were isolated and sequenced. One of the major AvrBsT-interacting proteins encoded ADC (four clones; Supplemental Figs. S1 and S2). This clone was designated *CaADC1* and used for further characterization. Other clones were also found to encode SGT1 (for suppressor of the G2 allele of *skp1*; three clones), HEAT SHOCK PROTEIN70 (three clones), and a putative aldehyde dehydrogenase (two clones; Kim, 2012).

To verify the interaction between AvrBsT and CaADC1, we swapped vectors and generated a DNA-binding domain (BD) fused with CaADC1 and an activation domain (AD) fused with AvrBsT. We transformed these constructs into yeast along with positive and negative control vector pairs. AD-AvrBsT and BD-CaADC1 pairs, and vice versa, interacted with each other and grew on synthetic dropout adenine, His, Leu, Trp medium (Fig. 1A).

The AvrBsT and CaADC1 interaction was verified in planta by using bimolecular fluorescence complementation (BiFC) assays (Walter et al., 2004). CaADC1 and AvrBsT were fused to the N-terminal 155-amino acid domain of yellow fluorescent protein (YFP) in the pSPYNE vector and the C-terminal 84-amino acid domain of YFP, respectively. *A. tumefaciens* cells harboring the corresponding constructs were mixed and coinfiltrated into *N. benthamiana* leaves. Confocal microscopy of *N. benthamiana* epidermal cells shows that AvrBsT and CaADC1 interact in the cytoplasm (Fig. 1B).

The AvrBsT and CaADC1 or CaADC1 K154A interaction in planta was investigated by coimmunoprecipitation using a transient coexpression system in *N. benthamiana* (Fig. 1C). Total proteins extracted from *N. benthamiana* leaves were incubated with anti-cMyc agarose to immunoprecipitate cMyc-tagged AvrBsT. Immunoprecipitates were resolved by SDS-PAGE. Immunoblotting using anti-cMyc antibody detected AvrBsT in the samples expressing AvrBsT alone and coexpressing AvrBsT:cMyc, CaADC1:hemagglutinin (HA), and CaADC1 K154A:HA. When immunoblotted using anti-HA, CaADC1, but not CaADC1 K154A, was detected from the samples coexpressing AvrBsT:cMyc

with CaADC1:HA or CaADC1 K154A:HA. Next, the total protein extracts were incubated with anti-HA agarose to immunoprecipitate HA-tagged CaADC1 or CaADC1 K154A. AvrBsT was immunodetected against anti-cMyc when coexpressed with CaADC1 but not with CaADC1 K154A or AvrBsT alone. Collectively, the coimmunoprecipitation assay revealed that AvrBsT forms a complex with CaADC1, but not with CaADC1 K154A, in planta.

Spatiotemporal Expression Profiles of *CaADC1*

RNA gel-blot analyses were used to investigate *CaADC1* expression profiles in pepper plants. *CaADC1* was constitutively expressed in stems, roots, flowers, and fruits but not in leaves (Supplemental Fig. S3A). Notably, *CaADC1* was highly induced in pepper leaves during avirulent (incompatible) *Xcv* infection compared with the mock control or the virulent (compatible) *Xcv* infection (Fig. 1D). In the incompatible interactions, *CaADC1* induction was detected 1 h after inoculation and reached a high level by 10 h after inoculation (Fig. 1D). Exogenous application of SA, methyl jasmonate, and ethylene also differentially induced *CaADC1* transcription in pepper leaves (Supplemental Fig. S3, B–D), indicating that *CaADC1* is involved in signal transduction pathways mediated by these plant hormones.

Transient Expression of *CaADC1* Specifically Promotes an *avrBsT*-Triggered Cell Death Response

To define the role of CaADC1 in the AvrBsT-triggered cell death response, we used an *A. tumefaciens*-mediated transient expression system in *N. benthamiana* leaves. As *CaADC1* expression was rapidly induced during the hypersensitive cell death response (Fig. 1D), we assumed that CaADC1 may function as a regulator of the cell death response. Because the activity of ADC requires the binding of pyridoxal phosphate at its Lys residue (Cohen et al., 1983), we performed site-directed mutagenesis to generate a *CaADC1 K154A* mutant that cannot bind pyridoxal phosphate. To determine whether *CaADC1* expression regulates the cell death response,

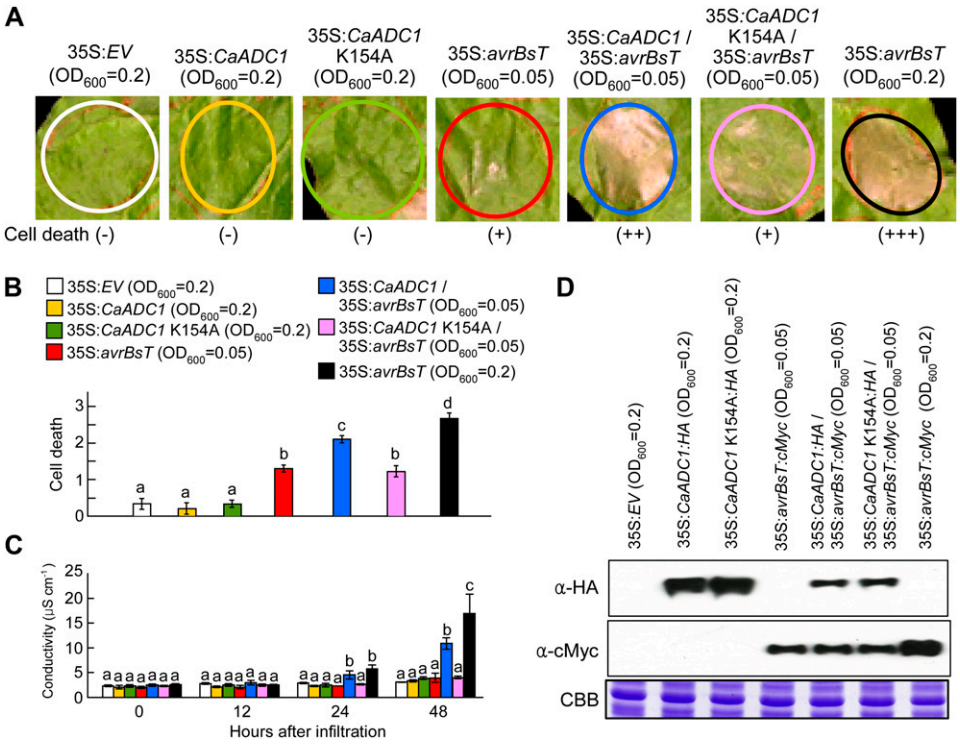

Figure 2. Transient expression of *CaADC1* promotes AvrBsT-triggered cell death. A, Cell death phenotypes. *N. benthamiana* leaves were infiltrated with *A. tumefaciens* carrying the indicated constructs at different inoculum ratios and photographed 2 d later. B, Cell death levels were rated based on a 0 to 3 scale: 0, no cell death (less than 10%); 1, weak cell death (10%–30%); 2, partial cell death (30%–80%); and 3, full cell death (80%–100%). Values represent averages of 10 samples. C, Electrolyte leakage from leaf discs at different time points after infiltration with *A. tumefaciens* carrying the indicated constructs at different inoculum ratios. Data are means ± SD from three independent experiments. Different letters indicate statistically significant differences (LSD; $P < 0.05$). D, Immunoblot analyses of the expression of 35S:*avrBsT*:*cMyc*, 35S:*CaADC1*:*HA*, and 35S:*CaADC1 K154A*:*HA*. Protein loading is visualized by Coomassie Brilliant Blue (CBB) staining. [See online article for color version of this figure.]

we coexpressed *CaADC1* or *CaADC1 K154A* with *avrBsT* at the lower limit of the cell death-inducing *A. tumefaciens* titer (optical density at 600 nm [OD_{600}] = 0.05). As shown in Figure 2A, transient expression of *CaADC1* or *CaADC1 K154A* did not induce a cell death phenotype in *N. benthamiana* leaves. At OD_{600} = 0.05, transient expression of *avrBsT* also did not trigger a full cell death response. However, coexpression of *avrBsT* with *CaADC1*, but not *CaADC1 K154A*, at OD_{600} = 0.05 produced a severely necrotic cell death phenotype that was similar to *avrBsT* expression at OD_{600} = 0.2 (Fig. 2, A and B). The extent of cell death was quantified by measuring electrolyte leakage from *N. benthamiana* leaves that were transiently expressing *CaADC1*, *CaADC1 K154A*, *avrBsT*, *CaADC1 K154A/avrBsT*, or *CaADC1/avrBsT*. Consistent with the visual cell death phenotypes, *CaADC1*-expressing leaf tissues exhibited very low levels of electrolyte leakage that were similar to those of the empty vector control and low-level expression of *avrBsT* (Fig. 2C). At 24 to 48 h after agroinfiltration, coexpression of *CaADC1* and *avrBsT* at the agrotiter of OD_{600} = 0.05 induced significantly higher electrolyte leakage than the expression of *avrBsT* alone at OD_{600} = 0.05. Coexpression of *CaADC1 K154A* and *avrBsT* at the agrotiter of OD_{600} = 0.05 showed a cell death phenotype and electrolyte leakage similar to that of expression of *avrBsT* alone at OD_{600} = 0.05. These results indicate that transient coexpression of the *CaADC1 K154A* mutant does not promote *avrBsT*-triggered cell death in *N. benthamiana* leaves. Immunoblot analyses confirmed that the epitope-tagged CaADC1, CaADC1 K154A, and AvrBsT proteins were transiently expressed in agroinfiltrated *N. benthamiana* leaves (Fig. 2D). For a specificity control, the mouse proapoptotic effector gene *BAX*, whose expression triggers cell death in plants (Lacomme and Santa Cruz, 1999; del Pozo et al., 2004), was coexpressed with *CaADC1* or *CaADC1 K154A* at the lower limit of the cell death-inducing *A. tumefaciens* titer (OD_{600} = 0.05). *CaADC1* or *CaADC1 K154A* coexpression did not promote a *BAX*-induced cell death response in *N. benthamiana* leaves (Supplemental Fig. S4, A and B). The *avrBsT* C222A mutant, which does not cause cell death in plants (Orth et al., 2000), was also coexpressed with *CaADC1* or *CaADC1 K154A*. The *CaADC1* or *CaADC1 K154A* coexpression in agroinfiltrated *N. benthamiana* leaves did not trigger cell death-inducing activity in AvrBsT C222A, although CaADC1 formed a complex with AvrBsT C222A (Supplemental Fig. S5, A and B). Collectively, these results indicate that *CaADC1* coexpression specifically promotes the *avrBsT*-triggered cell death response.

Effects of Transient Expression of *CaADC1* and *avrBsT* on PA Levels in *N. benthamiana* Leaves

Decarboxylation of Arg by ADC leads to the sequential formation of PAs such as putrescine, spermidine, and spermine (Flores and Filner, 1985). To investigate whether the transient expression of *CaADC1* and *avrBsT* affects

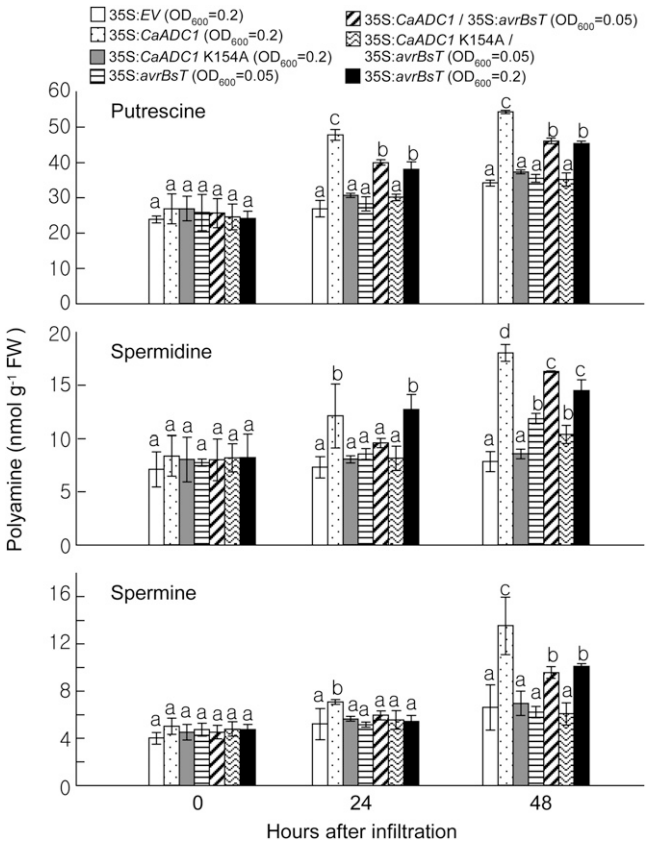

Figure 3. Effect of the transient expression of *CaADC1*, *CaADC1 K154A*, and *avrBsT* on PA levels in *N. benthamiana* leaves. Putrescine, spermidine, and spermine contents were determined in leaf tissues at 0, 24, and 48 h after *A. tumefaciens*-mediated transient expression of the indicated constructs. Data are means ± SD from three independent experiments. Different letters indicate statistically significant differences (LSD; $P < 0.05$). FW, Fresh weight.

PA metabolism, the levels of PAs were determined in *N. benthamiana* leaf tissues at 0, 24, and 48 h after *A. tumefaciens*-mediated transient expression of experimental constructs (Fig. 3). Transient expression of *CaADC1* resulted in increased accumulation of the three PAs at 24 h after agroinfiltration. The PAs remained at higher levels compared with those of the other constructs at 48 h after agroinfiltration. However, the *CaADC1 K154A* mutant did not exhibit induced accumulation of PAs, which was similar to the results with empty vector controls. Putrescine and spermidine were highly induced at 24 h after transient expression of *avrBsT* (OD_{600} = 0.2). By 48 h after agroinfiltration, the levels of the three PAs were significantly increased compared with those in the empty vector controls. At OD_{600} = 0.05, transient expression of *avrBsT* did not trigger the induction of PAs at 24 h after infiltration. However, coexpression of *avrBsT* with *CaADC1* at OD_{600} = 0.05 led to a significantly higher accumulation of putrescine at 24 h after agroinfiltration; by 48 h, all three PAs accumulated to levels that were similar to *avrBsT* expression at OD_{600} = 0.2. Coexpression

of *CaADC1 K154A* and *avrBsT* at the agrotiter of OD_{600} = 0.05 induced the accumulation of all three PAs, similar to the expression of *avrBsT* alone at OD_{600} = 0.05. Together, these data indicate that transient expression of *CaADC1*, *avrBsT*, or *CaADC1/avrBsT* induces PA accumulation in *N. benthamiana* leaves.

Effects of the Transient Expression of *CaADC1* and *avrBsT* on Amino Acid Levels in *N. benthamiana* Leaves

The catabolism of PAs produces GABA, which can be further metabolized to Glu or Ala (Bouché and Fromm, 2004). To analyze the effects of the transient expression of *CaADC1* and *avrBsT* on Arg and related amino acid levels, amino acid contents were determined in *N. benthamiana* leaves 1 and 2 d after infiltration of *A. tumefaciens* carrying 35S:*EV*, 35S:*CaADC1*, or 35S:*avrBsT* at OD_{600} = 0.2 (Supplemental Fig. S6). Transient expression of *ADC1* resulted in significantly lower levels of Arg and Ala, but not Glu or GABA, at 1 to 2 d after agroinfiltration. However, transient expression of *avrBsT* did not significantly alter levels of Glu, Arg, Ala, or GABA in *N. benthamiana*. These results indicate that transient expression of *CaADC1* reduces the accumulation of Arg and Ala in *N. benthamiana*.

Effects of *CaADC1* and *avrBsT* Transient Expression and PA Treatment on Nitric Oxide Production in *N. benthamiana* Leaves

There is evidence that nitric oxide (NO) and ROS bursts are involved in HR in plants (Asai et al., 2008; Yun et al., 2011). To investigate whether *CaADC1* and *avrBsT* transient expression and PA treatment induce the NO burst, NO was detected by 4,5-diaminofluorescein diacetate (DAF-2DA) staining of *N. benthamiana* leaves 24 h after infiltration with *A. tumefaciens* or PA (Fig. 4). Transient expression of *CaADC1* or *avrBsT* at OD_{600} = 0.2 markedly induced the NO burst, similar to that induced by the NO generator sodium nitroprusside (SNP; Fig. 4A). However, expression of *CaADC1 K154A* did not induce the NO burst, similar to the result with the empty vector control. NO induction by *avrBsT* expression at OD_{600} = 0.05 was significantly lower than that induced by the OD_{600} = 0.2 high-titer infiltration (Fig. 4A). Coexpression of *avrBsT* with *CaADC1*, but not with *CaADC1 K154A*, at OD_{600} = 0.05 induced significantly higher accumulation of NO than *avrBsT* alone at OD_{600} = 0.05.

To investigate whether PA application triggers the NO burst, putrescine, spermidine, and spermine were infiltrated into *N. benthamiana* leaves and NO accumulation was visualized 24 h after infiltration (Fig. 4B). As negative and positive controls, 10 mM $MgCl_2$ and 500 μM SNP were infiltrated into leaves, respectively. Infiltration of putrescine and spermidine at 1 mM did not significantly induce NO production; however, application of 1 mM spermine induced significantly higher NO production in *N. benthamiana* leaves.

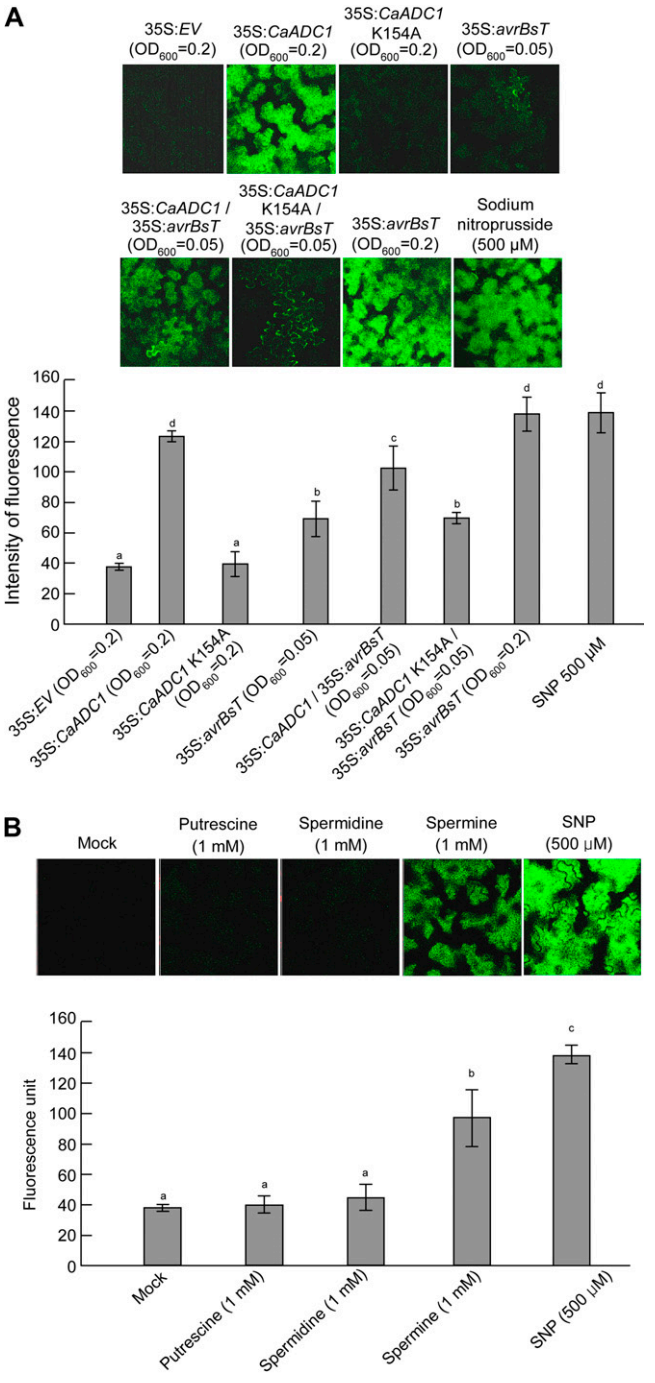

Figure 4. Quantification of the NO burst in *N. benthamiana* leaves 24 h after infiltration with either PAs or *A. tumefaciens* harboring the indicated constructs. Leaves were stained with DAF-FM DA and visualized with confocal microscopy. Signal intensities were quantified by color histogram analysis. Data are means ± SD from three independent experiments. Different letters indicate statistically significant differences (LSD; $P < 0.05$). A, Effect of the transient expression of *CaADC1*, *CaADC1 K154A*, or *avrBsT* on NO production. B, Effect of PA treatment on NO production. SNP (500 μm) treatment was used as a positive control. [See online article for color version of this figure.]

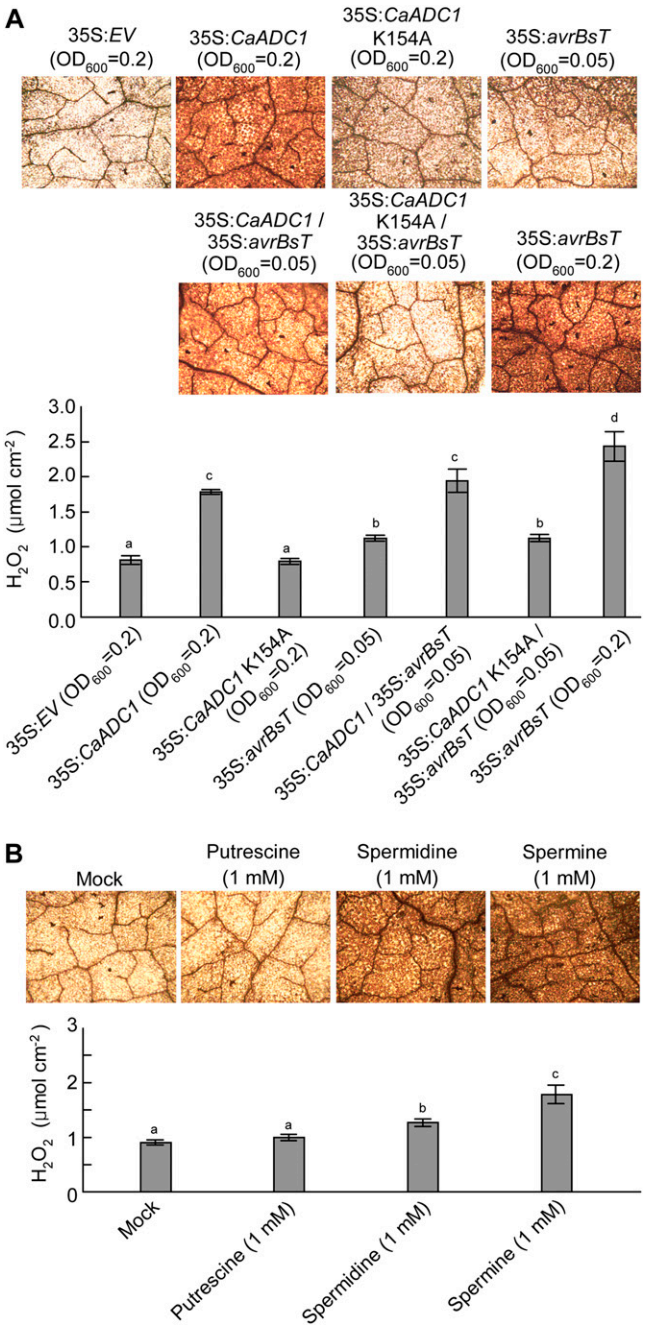

Figure 5. Quantification of the H_2O_2 burst in *N. benthamiana* leaves 24 h after infiltration with either PAs or *A. tumefaciens* harboring the indicated constructs. Leaves were stained with DAB. H_2O_2 concentrations were quantified by xylenol orange analysis. Data are means ± SD from three independent experiments. Different letters indicate statistically significant differences (LSD; $P < 0.05$). A, Effect of the transient expression of *CaADC1*, *CaADC1 K154A*, or *avrBsT* on H_2O_2 production. B, Effect of PA treatment on H_2O_2 production. The mock control was treated with 10 mM $MgCl_2$. [See online article for color version of this figure.]

Effects of *CaADC1* and *avrBsT* Transient Expression and PA Treatment on H_2O_2 Production in *N. benthamiana* Leaves

To investigate the effects of *CaADC1* and *avrBsT*-transient expression and PA treatments on the ROS burst in *N. benthamiana* leaves, H_2O_2 accumulation was visualized by 3,3′-diaminobenzidine (DAB) staining, and H_2O_2 levels were quantified by using the xylenol orange assay (Gay et al., 1999) 24 h after infiltration with *A. tumefaciens* or PA (Fig. 5). The H_2O_2 burst was distinctly induced by the transient expression of *CaADC1* or *avrBsT* at OD_{600} = 0.2 (Fig. 5A). However, expression of *CaADC1 K154A* did not induce the H_2O_2 burst, similar to the result with the empty vector control. At OD_{600} = 0.2, transient expression of *avrBsT* triggered higher H_2O_2 induction than did *avrBsT* expression at OD_{600} = 0.05. Coexpression of *avrBsT* with *CaADC1* at OD_{600} = 0.05 led to a significantly higher accumulation of H_2O_2 than did *avrBsT* alone at OD_{600} = 0.05. Coexpression of *CaADC1 K154A* and *avrBsT* at the agrotiter of OD_{600} = 0.05 induced H_2O_2 accumulation, similar to the expression of *avrBsT* alone at OD_{600} = 0.05.

To determine the effects of PAs on the H_2O_2 burst, putrescine, spermidine, and spermine at 1 mM were directly infiltrated into *N. benthamiana* leaves, and H_2O_2 was visualized 24 h after infiltration (Fig. 5B). Infiltration with 10 mM $MgCl_2$ was used as a mock control. Infiltration of 1 mM spermine resulted in the highest H_2O_2 accumulation. Spermidine also triggered significantly higher H_2O_2 accumulation as compared with the mock treatment. However, putrescine at 1 mM did not significantly induce the H_2O_2 burst (Fig. 5B).

Spermine Triggers Cell Death in *N. benthamiana* Leaves

The ability of spermine to trigger NO and H_2O_2 bursts (Figs. 4 and 5) prompted us to investigate whether PAs such as spermine function as positive triggers of cell death in plants. We infiltrated putrescine, spermidine, and spermine into *N. benthamiana* leaves using increasing concentrations from 0.5 to 10 mM (Fig. 6). For comparison, *A. tumefaciens* carrying 35S:*EV* and 35S:*avrBsT* was infiltrated at OD_{600} = 0.2 as negative and positive controls of cell death, respectively. Two days after infiltration, the empty vector control did not show any cell death response, whereas *avrBsT* transient expression induced hypersensitive cell death in *N. benthamiana* leaves (Fig. 6A). Surprisingly, infiltration of spermine at 10 mM induced a full necrotic cell death response, similar to that observed with *avrBsT* transient expression (Fig. 6, A and B). Infiltration of 10 mM putrescine or spermidine also triggered intermediate levels of cell death. The extent of cell death was quantified by measuring electrolyte leakage from *N. benthamiana* leaves infiltrated with 10 mM PAs. Among the PAs tested, spermine triggered the highest electrolyte leakage, similar to that resulting from *avrBsT* transient expression at 48 h after infiltration (Fig. 6C). The electrolyte leakage by putrescine infiltration

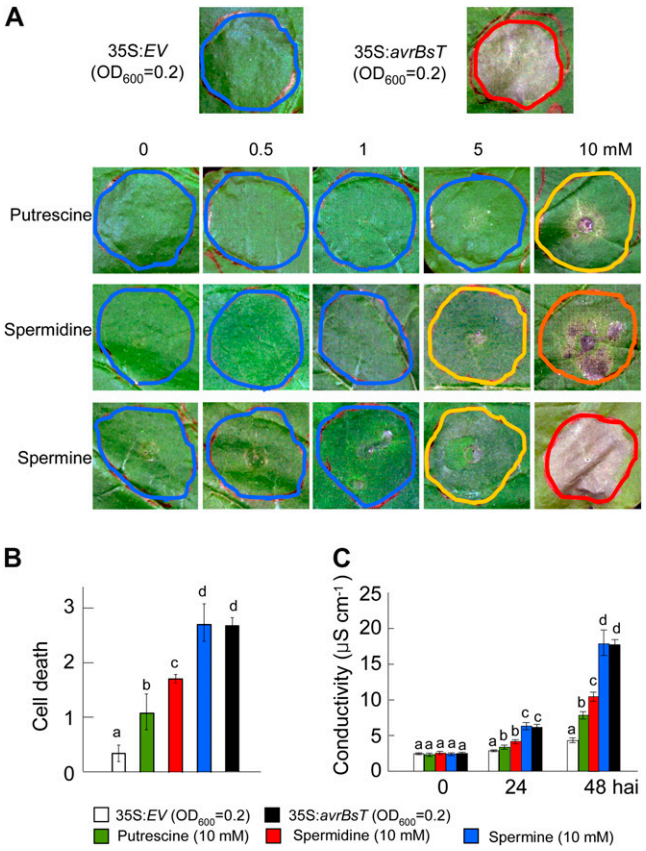

Figure 6. Effect of PA treatment on cell death response in *N. benthamiana* leaves. A, Cell death phenotypes in *N. benthamiana* leaves 2 d after infiltration with the indicated concentrations of putrescine, spermidine, or spermine. *A. tumefaciens* harboring 35S:*EV* or 35S:*avrBsT* was used as negative and positive controls, respectively. Red, orange, yellow, and blue circles indicate full, severe, partial, and no cell death, respectively. B, Quantification of cell death levels in leaves infiltrated with 10 mM PAs. Cell death levels were rated based on a 0 to 3 scale: 0, no cell death (less than 10%); 1, weak cell death (10%–30%); 2, partial cell death (30%–80%); and 3, full cell death (80%–100%). C, Electrolyte leakage from leaf discs at different time points after infiltration with 10 mM PAs. Data are means ± SD from three independent experiments. Different letters indicate statistically significant differences at different time points (Fisher's LSD; $P < 0.05$). [See online article for color version of this figure.]

was lower than that induced by spermidine but higher than that of the empty vector control (Fig. 6C). Collectively, these results indicate that spermine functions as a positive trigger of cell death in plants.

Spermine Promotes an *avrBsT*-Triggered Cell Death Response

To define the role of spermine in the *avrBsT*-triggered cell death response, we infiltrated 1 mM spermine mixed with *A. tumefaciens* carrying 35S:*EV*, 35S:*CaADC1*, 35S:*CaADC1 K154A*, or 35S:*avrBsT* into *N. benthamiana* leaves (Fig. 7). The control was infiltration of 10 mM $MgCl_2$ mixed with *A. tumefaciens* suspensions. Infiltration of *CaADC1* or *CaADC1 K154A* did not trigger cell death in *N. benthamiana* with or without 1 mM spermine (Fig. 7). Transient expression of *avrBsT* at OD_{600} = 0.05 was not able to trigger the full cell death response. However, addition of 1 mM spermine to *A. tumefaciens* carrying 35S:*avrBsT* at OD_{600} = 0.05 produced a severely necrotic cell death phenotype (Fig. 7, A and B). The extent of cell death was quantified by measuring electrolyte leakage from *N. benthamiana* leaves transiently expressing *CaADC1*, *CaADC1 K154A*, or *avrBsT* with or without 1 mM spermine. Consistent with the visual cell death phenotypes, very low levels of electrolyte leakage were observed in leaf tissues transiently expressing *CaADC1* or *CaADC1 K154A*, similar to that observed with the empty vector control. Addition of 1 mM

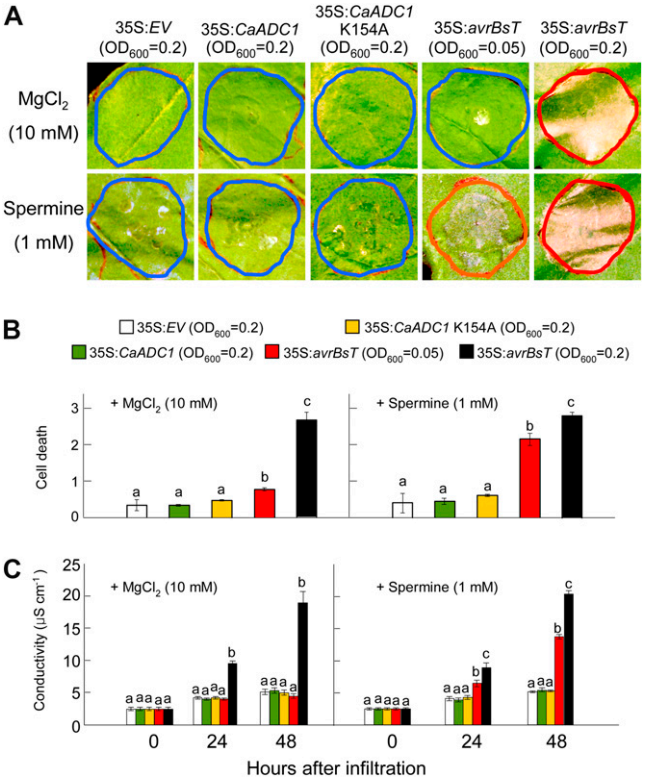

Figure 7. Spermine promotes AvrBsT-triggered cell death. A, Cell death phenotypes in *N. benthamiana* leaves 2 d after infiltration with *A. tumefaciens* carrying the indicated constructs and supplemented with 10 mM $MgCl_2$ or 1 mM spermine. Red, orange, and blue circles indicate full, severe, and no cell death, respectively. B, Quantification of cell death levels. Cell death levels were rated based on a 0 to 3 scale: 0, no cell death (less than 10%); 1, weak cell death (10%–30%); 2, partial cell death (30%–80%); and 3, full cell death (80%–100%). C, Electrolyte leakage from leaf discs at different time points after infiltration with *A. tumefaciens* carrying the indicated constructs and supplemented with 10 mM $MgCl_2$ or 1 mM spermine. Data are means ± SD from three independent experiments. Different letters indicate statistically significant differences at different time points (Fisher's LSD; $P < 0.05$). [See online article for color version of this figure.]

spermine to *A. tumefaciens* carrying 35S:*avrBsT* at OD_{600} = 0.05 induced higher electrolyte leakage than the empty vector control at 24 to 48 h after infiltration (Fig. 7C). Transient expression of *avrBsT* at the agrotiter of OD_{600} = 0.2 induced high levels of cell death phenotype and electrolyte leakage with or without spermine. Collectively, these results indicate that spermine positively regulates the *avrBsT*-triggered cell death response.

CaADC1 Is Required for the *avrBsT*-Triggered Cell Death Response to Incompatible *Xcv* Infection

We used the tobacco rattle virus (TRV)-based virus-induced gene silencing (VIGS) to investigate *CaADC1* loss of function in pepper plants (Liu et al., 2002). Leaves of empty vector (TRV:00) or silenced (TRV:*CaADC1*) pepper plants were inoculated with virulent (compatible) Ds1 (EV) or avirulent (incompatible) Ds1 (*avrBsT*) *Xcv* strains (10^7 and 10^8 colony-forming units [cfu] mL^{-1}). Silencing of *CaADC1* in pepper plants led to a highly susceptible response to incompatible *Xcv* infection (Supplemental Fig. S7). Inoculation with the avirulent Ds1 (*avrBsT*) *Xcv* strain (10^8 cfu mL^{-1}) caused cell death in the empty vector control leaves. However, HR-like cell death was not observed in *CaADC1*-silenced leaves 2 d after inoculation. Reduced cell death in leaves was more clearly noticeable, as observed under UV light (Supplemental Fig. S7). Incompatible *Xcv* Ds1 (*avrBsT*) growth in *CaADC1*-silenced leaves was approximately 10-fold higher than that in empty vector control leaves 3 d after inoculation (Fig. 8A). By contrast, no significant differences in compatible *Xcv* Ds1 (EV) growth were found between the empty vector control and silenced plants during infection. These results indicate that *CaADC1* is required for cell death-mediated resistance to *Xcv* infection.

Cell Death, ROS, and NO Bursts Are Compromised in *CaADC1*-Silenced Pepper

To investigate whether *CaADC1* regulates cell signaling pathways to induce early defense responses, we

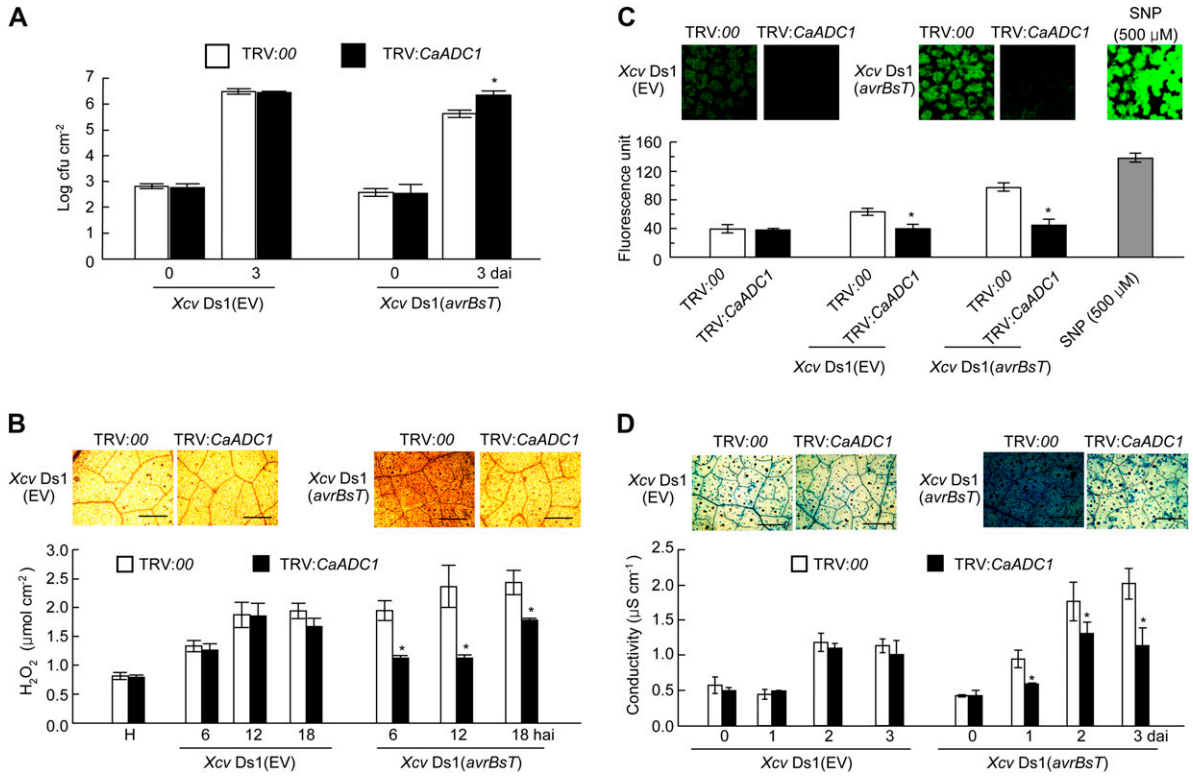

Figure 8. Enhanced susceptibility of *CaADC1*-silenced pepper plants to avirulent *Xcv* (*avrBsT*) infection. A, Bacterial growth in empty vector control and silenced leaves. Bacterial growth in leaves was measured at 0 and 3 d after inoculation with 5×10^4 cfu mL^{-1} *Xcv* Ds1 (EV) and *Xcv* Ds1 (*avrBsT*). B, DAB staining and H_2O_2 quantification at different time points after inoculation with 5×10^7 cfu mL^{-1} *Xcv* Ds1 (EV) and *Xcv* Ds1 (*avrBsT*). C, NO detection and relative intensity measurement by DAF-2DA staining. D, Trypan blue staining and electrolyte leakage measurement. Control (TRV:00) and *CaADC1*-silenced (TRV:*CaADC1*) leaves were inoculated with 5×10^7 cfu mL^{-1} *Xcv* Ds1 (EV) and *Xcv* Ds1 (*avrBsT*). Trypan blue staining was performed 24 h after infiltration, and electrolyte leakage was monitored at the indicated time points after infiltration. Data are means ± SD from three independent experiments. Asterisks indicate statistically significant differences (Student's *t* test; $P < 0.05$). H, Healthy leaves. [See online article for color version of this figure.]

analyzed and compared ROS (H_2O_2) and NO accumulation and cell death response in empty vector control and *CaADC1*-silenced pepper leaves during *Xcv* infection (Fig. 8, B–D). H_2O_2 and NO production and cell death were visualized by DAB, DAF-2DA, and trypan blue staining, respectively. Significantly compromised H_2O_2 and NO accumulation and cell death response were observed in the *CaADC1*-silenced leaves inoculated with incompatible *Xcv* Ds1 (*avrBsT*). Xylenol orange assay, relative intensity of DAF-2DA signals, and ion conductivity measurements were used to quantify H_2O_2 and NO production and cell death, respectively. Silencing of *CaADC1* significantly compromised the accumulation of H_2O_2 and NO and lowered ion leakage in pepper leaves during the incompatible *Xcv* (*avrBsT*) infection. NO accumulation was also significantly compromised by *CaADC1* silencing during the compatible *Xcv* infection and remained at the basal level.

CaADC1 Expression Positively Regulates SA-Induced Defense Genes

To determine whether *CaADC1* silencing alters the expression of pepper defense-related genes at early infection stages, real-time reverse transcription (RT)-PCR analyses were performed using gene-specific primer pairs for *CaADC1*, *CaPR1*, *CaPR10*, and *CaDEF1* (for defensin; Supplemental Table S1) at 1 and 2 d after inoculation with the compatible *Xcv* Ds1 (EV) and incompatible *Xcv* Ds1 (*avrBsT*) strains (Fig. 9A). *CaADC1* silencing in pepper leaves significantly compromised induction of the SA-induced defense genes *CaPR1* and *CaPR10*, but not the jasmonate-related gene *CaDEF1*, during the incompatible *Xcv* infection. By contrast, consistently compromised induction of these defense-related genes was not detected in *CaADC1*-silenced leaves that were infected by the compatible *Xcv* Ds1 (EV) strain. Collectively, these results suggest the involvement of *CaADC1* in defense signaling mediated by SA during incompatible interactions of *Xcv* with pepper.

Accumulation of SA Is Compromised in *CaADC1*-Silenced Pepper during Incompatible *Xcv* Infection

To determine if *CaADC1* silencing regulates SA signaling in the defense response to bacterial infection, we quantified the levels of free and total SA in empty vector control and *CaADC1*-silenced pepper leaves during *Xcv* infection (Fig. 9B). Accumulation of free and total SA (free SA plus Glc-conjugated SA) significantly declined in *CaADC1*-silenced leaves compared with empty vector control leaves at 1 and 2 d after incompatible *Xcv* infection. In contrast, *CaADC1* silencing did not affect SA accumulation during compatible *Xcv* infection.

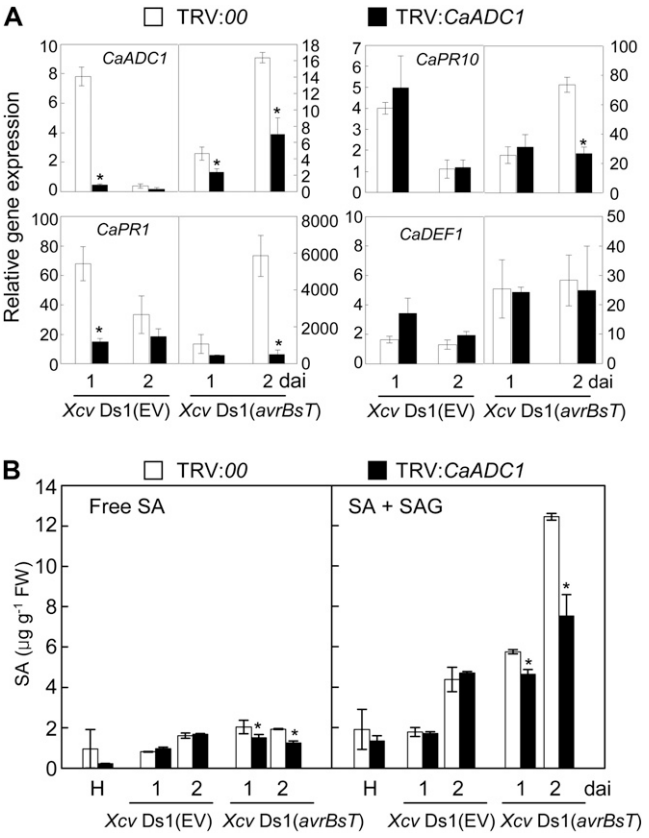

Figure 9. *CaADC1* silencing compromises SA-dependent defense gene expression and SA accumulation in pepper leaves infected with *Xcv*. A, Expression profiles of defense-related genes. B, Free and total SA levels in empty vector control (TRV:00) and *CaADC1*-silenced (TRV:*CaADC1*) pepper leaves infected by *Xcv*. Total RNA was isolated from empty vector control (TRV:00) and *CaADC1*-silenced (TRV:*CaADC1*) pepper leaves inoculated with 5×10^7 cfu mL^{-1} of the *Xcv* strains Ds1 (EV) and Ds1 (*avrBsT*). Quantitative real-time PCR was performed for *CaADC1* and pepper *PR* genes: *CaPR1*, *CaPR10*, and *CaDEF1*. Relative expression levels at 1 and 2 d after inoculation (dai) are shown. Relative expression values are normalized to the expression of pepper 18S ribosomal RNA in each sample. SA contents were determined in empty vector control and silenced leaves at 1 and 2 d after inoculation with *Xcv*. Data are means ± SD from three independent experiments. Asterisks indicate significant differences as determined by Student's *t* test ($P < 0.05$). FW, Fresh weight.

CaADC1 Silencing Compromises PA Accumulation in Pepper during Incompatible *Xcv* Infection

To investigate whether the silencing of *CaADC1* affects PA metabolism, the levels of putrescine, spermidine, and spermine were determined in empty vector control and *CaADC1*-silenced pepper leaves at 1 and 2 d after *Xcv* inoculation (10^7 cfu mL^{-1}; Fig. 10). In empty vector control leaves, putrescine and spermidine levels were greatly increased by both *Xcv* Ds1 (EV) and *Xcv* Ds1 (*avrBsT*) infection. Interestingly, the levels of spermine were only increased by avirulent *Xcv* Ds1 (*avrBsT*) infection. In contrast, *CaADC1* silencing compromised the accumulation of putrescine,

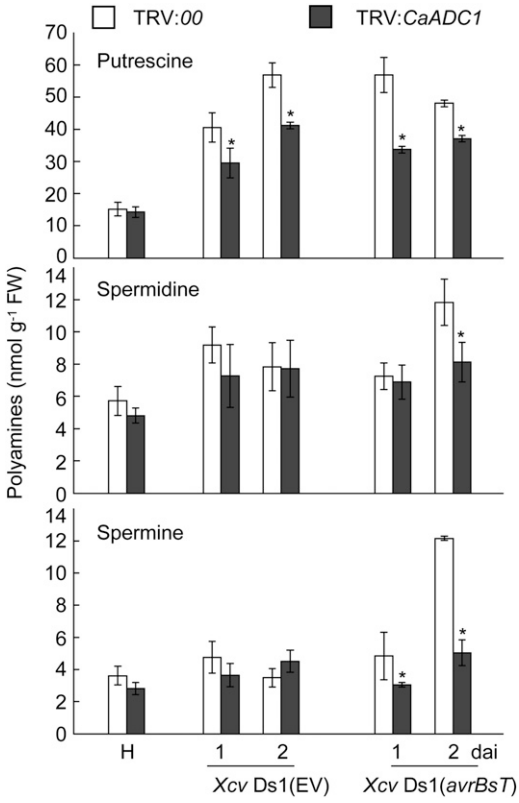

Figure 10. Levels of putrescine, spermidine, and spermine in leaves of empty vector control (TRV:00) and *CaADC1*-silenced (TRV:*CaADC1*) pepper plants infected with 10^7 cfu mL^{-1} of the virulent Ds1 (EV) and avirulent Ds1(*avrBsT*) strains of *Xcv*. Data are means ± SD from three independent experiments. Asterisks indicate statistically significant differences (Student's *t* test; $P < 0.05$). FW, Fresh weight; H, healthy leaves.

spermidine, and spermine in pepper leaves during avirulent *Xcv* Ds1 (*avrBsT*) infection. However, virulent *Xcv* Ds1 infection compromised putrescine accumulation in *CaADC1*-silenced pepper leaves but did not distinctly affect the contents of spermidine and spermine in empty vector control and *ADC1*-silenced pepper leaves.

CaADC1 Silencing Compromises the Accumulation of Gln, Ala, and GABA in Pepper Leaves

To determine whether the silencing of *CaADC1* affects levels of Arg and related amino acids, free amino acids levels of Gln, Arg, Ala, and GABA were compared in empty vector control (TRV:00) and *CaADC1*-silenced leaves during incompatible *Xcv* infection (Fig. 11A; Supplemental Fig. S8). There were no significant differences in the levels of Arg between empty vector control and *CaADC1*-silenced leaves. However, decreased Ala and Glu levels were detected in *CaADC1*-silenced leaves compared with empty vector control leaves during both *Xcv* Ds1 (EV) and *Xcv* Ds1 (*avrBsT*) infection. Notably, *CaADC1* silencing significantly compromised GABA accumulation in pepper leaves during avirulent *Xcv* Ds1 (*avrBsT*) infection. Together, these results indicate that CaADC1 plays a crucial role in the accumulation of Gln, Ala, and GABA during *Xcv* Ds1 (*avrBsT*) infection.

GABA Promotes Resistance against *Xcv* Ds1 (*avrBsT*) Infection

We investigated whether the application of exogenous Ala or GABA affects resistance against *Xcv* infection in pepper leaves. The addition of Ala or GABA to the culture medium did not have any positive or adverse effect on *Xcv* growth (Supplemental Fig. S9). Empty vector control and *CaADC1*-silenced pepper leaves were infiltrated with 10 mM $MgCl_2$ (mock),

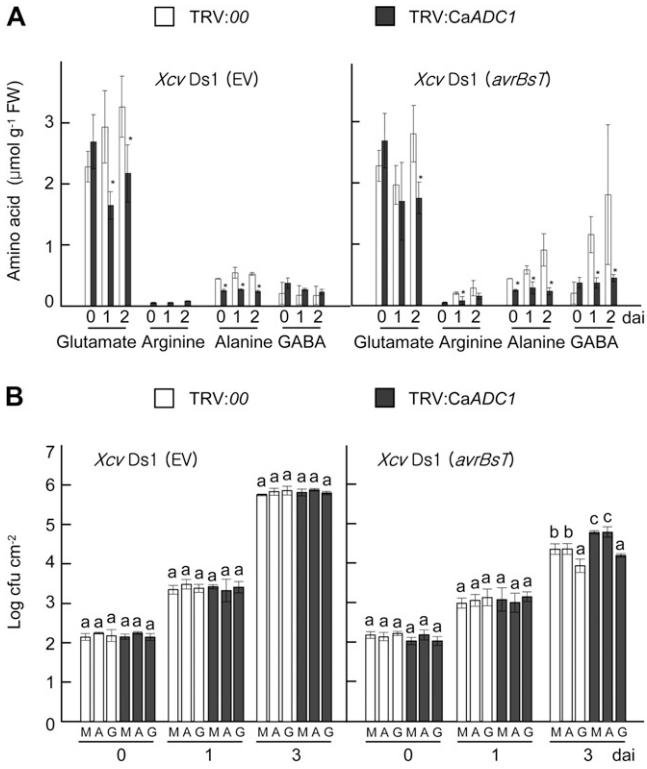

Figure 11. GABA suppresses *Xcv* growth in pepper leaves. A, Levels of amino acids in leaves of empty vector control (TRV:00) and *CaADC1*-silenced (TRV:*CaADC1*) pepper plants infected with 10^7 cfu mL^{-1} of the virulent Ds1 (EV) and avirulent Ds1 (*avrBsT*) strains of *Xcv*. Data are means ± SD from three independent experiments. Asterisks indicate statistically significant differences (Student's *t* test; $P < 0.05$). B, Exogenous application of GABA suppresses the proliferation of avirulent *Xcv* Ds1 (*avrBsT*) in leaves of empty vector control and *CaADC1*-silenced plants. Leaves were treated with 10 mM $MgCl_2$ (mock [M]), Ala (A), or GABA (G) 1 d before infiltration with 5×10^4 cfu mL^{-1} *Xcv* Ds1 (EV) and Ds1 (*avrBsT*). Data are means ± SD. Different letters indicate statistically significant differences (LSD; $P < 0.05$). FW, Fresh weight.

10 mM Ala, or 10 mM GABA 1 d prior to *Xcv* inoculation, and bacterial growth was monitored at 0, 1, and 3 d after *Xcv* inoculation (Fig. 11B). Treatment with Ala did not suppress the growth of compatible *Xcv* Ds1 (EV) and incompatible Ds1 (*avrBsT*) in empty vector control and *CaADC1*-silenced pepper leaves. However, GABA treatment of empty vector control and *CaADC1*-silenced pepper leaves significantly reduced avirulent *Xcv* Ds1 (*avrBst*) growth 3 d after inoculation (Fig. 11B). These results suggest that GABA enhances cell death-mediated resistance against *Xcv* at a late infection stage.

DISCUSSION

Pepper plants recognize the type III effector protein AvrBsT that is secreted by *Xcv* and respond by triggering the cell death response (Escolar et al., 2001; Kim et al., 2010). The involvement of phosphatidic acids in the AvrBsT-triggered cell death was revealed by the identification of SUPPRESSOR OF AVRBST-ELICITED RESISTANCE1, a conserved carboxylesterase of the Arabidopsis Pi-0 ecotype (Cunnac et al., 2007; Kirik and Mudgett, 2009). In pepper, AvrBsT was found to target a putative regulator of sugar metabolism, SNF1-RELATED KINASE1, which is required for AvrBs1-induced immunity (Szczesny et al., 2010). However, the cognate R proteins for AvrBsT have not yet been identified. To better understand the molecular mechanisms underlying AvrBsT-triggered cell death in pepper plants, we have identified CaADC1 as an AvrBsT-interacting protein.

AvrBsT has been proposed to localize at the cytoplasm and nucleus (Szczesny et al., 2010). The in vitro and in planta interactions between AvrBsT and CaADC1 were revealed using yeast two-hybrid, BiFC, and coimmunoprecipitation assays. These data suggest that the interaction of AvrBsT with CaADC1 occurs at the cytoplasm only when CaADC1 is in the active state. The inactive CaADC1 K154A mutant that cannot bind to the essential coenzyme, pyridoxal phosphate (Cohen et al., 1983), did not interact with AvrBsT, which could not ultimately enhance the AvrBst-triggered cell death response in *N. benthamiana* leaves. However, the cell death-inactive AvrBsT C222A mutant was able to bind to CaADC1. Interestingly, coexpression of the CaADC1 that was only able to bind to AvrBsT specifically enhanced AvrBsT-triggered cell death. Collectively, these results suggest that CaADC1 acts as a positive regulator of cell death signaling in plants.

Coexpression of AvrBsT with CaADC1 significantly enhanced the cell death phenotype and concurrently increased electrolyte leakage. This enhancement effect may be dependent on the ADC activity of CaADC1, because the *CaADC1 K154A* mutant did not undergo cell death triggered by AvrBsT. Moreover, the CaADC1 enhancement effect was specific to AvrBsT, as *CaADC1* coexpression did not promote *BAX*-induced cell death. *CaADC1* expression induced an overaccumulation of PAs, and the results demonstrate that spermine could induce NO and H_2O_2 bursts that lead to cell death. During the resistance response of barley (*Hordeum vulgare*) to powdery mildew (*Blumeria graminis* f. sp. *hordei*), ODC or ADC activities greatly increased and resulted in higher PA levels (Cowley and Walters, 2002). However, *ODC* genes are proposed to be absent in Arabidopsis (Hanfrey et al., 2001). This suggests a predominant role for ADC in PA metabolism, at least in Arabidopsis. Similarly, significantly higher spermine levels accumulated in tobacco (*Nicotiana tabacum*) plants due to increased ADC activity during *Pseudomonas viridiflava* infection, suggesting a beneficial role of ADC for the defense against the pathogen (Marina et al., 2008).

The PA catabolism mediated by NADPH oxidases or peroxidases is a major source of the ROS burst (Takahashi et al., 2004). ROS have widely been known to be crucial for various plant defense responses, such as cell wall strengthening, defense gene activation, and cell death and systemic acquired resistance induction (Lamb and Dixon, 1997; Torres et al., 2006; Van Breusegem and Dat, 2006). Exogenous application of PAs to Arabidopsis seedlings induced NO production (Wimalasekera et al., 2011). However, the processes in which the NO is produced in response to increased PA levels remain unclear (Yamasaki and Cohen, 2006). The nitrate reductase is only an enzyme required to produce NO (Rockel et al., 2002; Moreau et al., 2010). More recently, it has been demonstrated that PAs could increase nitrate reductase activity in wheat (*Triticum aestivum*; Rosales et al., 2012), suggesting an indirect role for PAs to generate NO. Whether an oxidative way is required to produce NO from the substrates, such as Arg, PA and hydroxylamines are actively being investigated (Besson-Bard et al., 2008; Moreau et al., 2010). NO has been shown to play essential roles in animal innate immune and inflammatory responses, and several downstream targets of NO, such as guanylate cyclase and mitogen-activated protein kinases, are shared by both animals and plants (Klessig et al., 2000). Recently, *S*-nitrosylation of NADPH oxidase was proposed to regulate cell death in plant immunity (Yun et al., 2011).

More importantly, the experimental evidence that the addition of 1 mM spermine to *A. tumefaciens* carrying *35S:avrBsT* could promote AvrBsT-triggered cell death in inoculated leaves supports the hypothesis that *CaADC1* expression induces the production of PAs such as spermine to trigger the cell death response in plants. The involvement of spermine in defense and cell death responses has been demonstrated in other plant-pathogen systems (Mitsuya et al., 2009; Gonzalez et al., 2011). In tobacco, treatment with spermine induced the activation of mitogen-activated protein kinases through mitochondrial dysfunction (Takahashi et al., 2003). A subset of hypersensitive response marker genes is proposed to be the downstream target of a spermine signal transduction pathway in plants (Takahashi et al., 2004). Interestingly, spermine was

demonstrated to induce cell death in human embryonic cerebral cortical neurons and mouse melanoma cells (Averill-Bates et al., 2008; de Vera et al., 2008).

In contrast to the promotion of cell death by transient expression of *CaADC1*, *avrBsT*-triggered cell death was compromised in *CaADC1*-silenced pepper leaves, as shown by decreased electrolyte leakage. *CaADC1* silencing in pepper leaves significantly compromised the induction of H_2O_2, SA, and SA-dependent *CaPR1* and *CaPR10* defense genes during avirulent *Xcv* infection. SA plays a pivotal role for plant inducible immunity (Du et al., 2009; Tsuda et al., 2009). Furthermore, *CaADC1*-silenced pepper leaves contained significantly lower levels of spermine and GABA. The signaling and metabolic changes that affect defense and cell death responses in *CaADC1*-silenced pepper leaves may be primarily due to the reduced expression of *CaADC1*. ADC functions as a rate-limiting factor that regulates PA levels in plants (Kasinathan and Wingler, 2004; Alcázar et al., 2005). PA catabolic processes directly produce H_2O_2 (Bagni and Tassoni, 2001), which is consistent with the reduced levels of H_2O_2 that were observed in *CaADC1*-silenced pepper leaves. It has been suggested that the H_2O_2 burst is linked to HR and the defense hormone SA accumulation (Durrant and Dong, 2004; Torres et al., 2006). More importantly, *CaADC1* silencing significantly compromised avirulent *Xcv* Ds1 (*avrBsT*) proliferation in pepper leaves during infection. The increased *Xcv* Ds1 (*avrBsT*) growth in *CaADC1*-silenced pepper leaves supports the notion that CaADC1 interacts with AvrBsT and enhances AvrBsT-triggered cell death resistance, ultimately to the inhibition of *Xcv* Ds1 (*avrBsT*) proliferation in the incompatible interaction of pepper plants.

The AvrBsT-triggered cell death resistance conferred by *CaADC1* expression may be, in part, related to GABA. During the avirulent *Xcv* Ds1 (*avrBsT*) infection, but not the *Xcv* Ds1 (EV) infection, *CaADC1* silencing did not induce GABA accumulation compared with the empty vector control plants. As a result, *CaADC1*-silenced plants were more susceptible to avirulent *Xcv* Ds1 (*avrBsT*) but not to virulent *Xcv* Ds1 (EV). In addition, exogenous application of GABA significantly reduced avirulent *Xcv* Ds1 (*avrBsT*) growth in the empty vector control and *CaADC1*-silenced pepper leaves. Together, these results strongly suggest that the nonprotein amino acid GABA may contribute to AvrBsT-triggered cell death-like resistance against *Xcv* infection. As a remarkably versatile signaling molecule, GABA has been proposed to mediate communication between plants and other organisms, including bacterial and fungal pathogens, nematodes, and insect pests (Shelp et al., 2006). Accumulation of GABA in tobacco plants induces quenching of quorum-sensing in *A. tumefaciens*, thereby attenuating its virulence on plants (Chevrot et al., 2006). Mutations in GABA transaminase genes in plants or *Pseudomonas syringae* reduces bacterial virulence (Park et al., 2010), suggesting the role of GABA in plant defense response to pathogenic bacteria. There is evidence that GABA is linked to ROS generation and cell death in plants (Bouché et al., 2003). The GABA isomer, β-aminobutyric acid, has been shown to induce disease resistance in Arabidopsis against *Alternaria brassicicola* and *Plectosphaerella cucumerina* (Ton and Mauch-Mani, 2004). GABA is known to be accumulated in plants to counteract abiotic and biotic stresses (Choi et al., 2004; Lima et al., 2010). Like these previous findings, our data support the role of GABA as an active defense inducer in plants.

In summary, these data provide novel information regarding AvrBsT-triggered cell death in pepper plants that is positively regulated by CaADC1. We propose a working model based on these results in which CaADC1 plays a pivotal role in PA and GABA signaling in defense responses in plants (Supplemental Fig. S10). AvrBsT induces *CaADC1* expression, interacts with CaADC1, and presumably activates CaADC1. Active CaADC1 catalyzes the synthesis of agmatine, which is further metabolized to produce putrescine (Bagni and Tassoni, 2001). Spermidine is synthesized from putrescine via the addition of aminopropyl groups to putrescine by spermidine synthase (Bagni and Tassoni, 2001; Walters, 2003b), followed by the production of H_2O_2 as a by-product. Spermine is synthesized via the addition of aminopropyl groups to spermidine by spermine synthase (Bagni and Tassoni, 2001), leading to the production of H_2O_2. In addition, spermine can directly trigger a NO burst. PAs also can be catabolized to pyrroline, which is further processed to form GABA (Flores and Filner, 1985). GABA is proposed to contribute to defense responses by affecting the ROS burst during pathogen infection (Bouché et al., 2003). The ROS and NO bursts induced by PAs may activate downstream signaling pathways, such as mitogen-activated protein kinase cascades (Wang et al., 2010). ROS are involved in SA signaling, which regulates cell death and defense responses in plants (Torres et al., 2006). In conclusion, these results suggest that CaADC1 may act as a key regulator of cell death and defense signaling and contribute to disease resistance by fine-tuning PA and GABA levels in pepper plants.

MATERIALS AND METHODS

Plant Materials and Pathogen Inoculation

Pepper (*Capsicum annuum* 'Nockwang') and *Nicotiana benthamiana* were grown in plastic pots (8 cm in diameter) containing a soil mix (loam soil: perlite:vermiculite, 3:1:1, v/v/v) at 28°C with long-day cycles (16 h of light and 8 h of dark) at a light intensity of 100 μmol photons m^{-2} s^{-1}.

The *Xanthomonas campestris* pv *vesicatoria* virulent Ds1 (EV) and avirulent Ds1 (*avrBsT*) strains (Kim et al., 2010) were grown overnight in yeast nutrient medium (5 g L^{-1} yeast extract and 8 g L^{-1} nutrient broth), harvested, and then resuspended in 10 mM $MgCl_2$ solution. Bacterial growth in leaves was monitored at 0 and 3 d after infiltration with *Xcv* (5×10^4 cfu mL^{-1}) using a syringe (without needle).

Yeast Two-Hybrid Assays

The open reading frame of the *Xcv* type III effector protein gene *avrBsT* was cloned into the pGBKT7 (*Bam*HI/*Hin*dIII sites) vector. A yeast prey library was generated from a pepper cDNA library by ligating cDNA inserts with the

pGADT7 vector. The constructs were cotransformed into yeast strain AH109 and plated onto synthetic dropout His, Leu, Trp medium (Ito et al., 1983). Approximately 50,000 colonies grown on synthetic dropout His, Leu, Trp medium were transferred onto selection medium (synthetic dropout adenine, His, Leu, Trp medium). Plasmids were extracted from surviving yeast colonies and used to transform *Escherichia coli*. Colonies carrying the pGADT7 vector were selected on Luria-Bertani medium containing 100 mg L^{-1} ampicillin. Isolated plasmids were sequenced, and sequence homology was analyzed using GenBank BLAST tools.

BiFC Assay

The BiFC assay was conducted as described previously (Walter et al., 2004). To generate the BiFC constructs, cDNAs encoding AvrBsT and CaADC1 without termination codons were PCR amplified and subcloned into the binary vectors pSPYNE (*Xba*I/*Xho*I) and pSPYCE (*Xba*I/*Xho*I) vectors under the control of the cauliflower mosaic virus 35S promoter (for oligonucleotide sequences, see Supplemental Table S2). pSPYCE:*CaADC1 K154A* was generated using the QuickChange site-directed mutagenesis kit (Stratagene). *AvrBsT* and *CaADC1* were coexpressed in *Nicotiana benthamiana* leaves by infiltrating *Agrobacterium tumefaciens* strain GV3101 carrying each construct (OD_{600} = 0.5). The association of AvrBsT and CaADC1 was visualized using a confocal laser scanning microscope (LSM 5 Exciter; Carl-Zeiss) operated with the LSM Imager at 40 h after transformation.

VIGS

TRV-based VIGS was used to generate *CaADC1* knockdown pepper plants (Liu et al., 2002; Choi et al., 2007). The unconserved 3′ region of the *CaADC1* untranslated region was PCR amplified using the primers listed in Supplemental Table S2. The resulting fragment was cloned into pCR2.1/TOPO, digested with *Eco*RI, and inserted into pTRV2 (*Eco*RI/*Eco*RI). The fully expanded cotyledons of pepper plants were coinfiltrated with *A. tumefaciens* strain GV3101 carrying the VIGS vectors pTRV1 and pTRV2 or pTRV2:*CaADC1* (OD_{600} = 0.2). The efficacy of *CaADC1* silencing in pepper plants was examined by RT-PCR after *Xcv* inoculation at the six-leaf stage.

RNA Gel-Blot and Real-Time RT-PCR Analyses

Total RNA was extracted from pepper plants using Trizol reagent (Invitrogen). RNA was resolved by agarose gel electrophoresis, transferred onto Hybond N^+ membranes (GE Healthcare), and hybridized overnight with ^{32}P-labeled *CaADC1* cDNA.

For real-time RT-PCR, 2 μg of RNA were used in a RT reaction with Moloney murine leukemia virus reverse transcriptase (Enzynomics). Real-time PCR was performed using iQ SYBR Green Supermix and iCycler iQ (Bio-Rad). The 18S ribosomal RNA transcript level was used to normalize the transcript level of each gene. Relative expression levels were determined by comparing the values with that of the uninoculated control.

Coimmunoprecipitation and Immunoblot Analyses

For coimmunoprecipitation constructs, *avrBsT* and *CaADC1* were PCR amplified using the primers listed in Supplemental Table S2. The fragments were digested with *Xba*I/*Xho*I and ethanol precipitated. Digested *avrBsT* and *CaADC1* fragment was recombined into p35S:8xMyc and p35S:6xHA, respectively (Choi et al., 2012). *A. tumefaciens* strain GV3101 harboring the constructs was coinfiltrated into *N. benthamiana* leaves. Proteins were extracted from leaf samples using extraction buffer (50 mM Tris-HCl, pH 7.5, 150 mM NaCl, 10 mM EDTA, 0.2% (v/v) Triton X-100, and 2× complete protease inhibitor cocktail [Roche]). The protein extracts were incubated with monoclonal anti-HA or anti-Myc agarose (Sigma-Aldrich) overnight. Beads were collected and washed with immunoprecipitation buffer (50 mM Tris-HCl, pH 7.5, 150 mM NaCl, 10 mM EDTA, and 2× complete protease inhibitor cocktail [Roche]). Eluted proteins were analyzed by immunoblotting using monoclonal anti-HA-peroxidase antibody (Sigma-Aldrich) or polyclonal anti-cMyc-peroxidase antibody (Sigma-Aldrich). Immunodetection was performed using the ECL Prime Western Blotting Detection Reagent (GE Healthcare).

Ion Leakage Assay

Leaves of *N. benthamiana* or pepper plants were harvested at various time points after infiltration with *A. tumefaciens* or *Xcv*. Leaf discs (0.5 cm in diameter) were removed with a cork borer and washed in 10 mL of sterile double-distilled water for 30 min with gentle agitation. Washed leaf discs were transferred to 20 mL of sterile double-distilled water and incubated for 2 h at room temperature with gentle agitation. The conductivity of the leaf samples was measured using a Sension 7 conductivity meter (HACH). Experiments were carried out three times with similar results.

SA Measurement

SA levels in pepper leaves were determined as described previously (Choi and Hwang, 2011). Leaf tissues (0.5 g) were homogenized in liquid nitrogen and extracted in 1 mL of 90% (v/v) methanol. The leaf extracts were then centrifuged at 15,000*g* for 5 min. The resulting pellet was reextracted with 100% methanol. The supernatant fractions were then pooled and vacuum dried. The residue was resuspended in 1 mL of 5% (v/v) TCA. Organic extraction of free SA was performed following the addition of 1 mL of ethyl acetate:cyclopentane:isopropanol (50:50:1). The aqueous phase was then reextracted with ethyl acetate:cyclopentane:isopropanol, and the two organic phases were pooled and vacuum dried. The pellet was resuspended in 1 mL of 100% methanol. The suspension was centrifuged at 15,000*g* for 2 min and filtered through a 0.2-μm Acrodisc syringe filter (PALL). The aqueous phase containing the SA glucoside fraction was acidified with HCl to pH 1 and boiled for 30 min to release SA from any acid-labile conjugated forms. The released SA was extracted with ethyl acetate:cyclopentane:isopropanol, vacuum dried, and resuspended in 1 mL of 100% methanol. 3-Hydroxybenzoic acid (50 μg per leaf sample) was used as an internal standard. SA in the extracts was analyzed by reverse-phase HPLC in a Waters 515 system using a C18 column. SA in the eluates was detected by passage through a fluorescence detector (excitation at 305 nm and emission at 405 nm).

Histochemical Analyses

H_2O_2 production was visualized by placing healthy or inoculated leaves in 1 mg mL^{-1} DAB (Sigma-Aldrich) solution for 15 h (Thordal-Christensen et al., 1997). Chlorophyll was cleared from the stained leaves by boiling in 95% (v/v) ethanol. Cell death was monitored by trypan blue staining of healthy or inoculated leaves (Koch and Slusarenko, 1990). Leaves were stained with lactophenol-trypan blue solution (10 mL of lactic acid, 10 mL of glycerol, 10 g of phenol, and 10 mg of trypan blue, dissolved in 10 mL of distilled water) and destained in 2.5 g mL^{-1} chloral hydrate solution. The samples were photographed using a light microscope mounted with a digital camera (Olympus). Chlorosis, cell death, or phenolic compound accumulation in leaves was visualized using a hand-held UV lamp (UVP).

PA Measurement

PA accumulation was monitored using a gas chromatography-mass spectrometry method as described previously (Chen et al., 2009). Briefly, 100-mg leaf samples were homogenized and extracted with 1 mL of 10% (v/v) NaCl (pH 1) and centrifuged at 12,000*g* for 15 min. The resulting supernatants were extracted with 3 mL of diethyl ether by vortexing for 10 min and centrifuged at 12,000*g* for 20 min. Aliquots (0.5 mL) of the samples were adjusted to pH 10 with 5 M NaOH and mixed with 1 mL of diethyl ether containing 50 μL of ethyl chloroformate by shaking for 30 min at room temperature. The mixture was centrifuged at 12,000*g* for 5 min, and the ether layer containing the PA *N*-ethoxylcarbonyl derivatives was transferred to a separate glass vial and dried under a nitrogen stream. Ethyl acetate (100 μL) was added to the dried *N*-ethoxylcarbonyl PA derivatives, mixed with 200 μL of trifluoroacetic acid anhydride, and incubated at 75°C for 1 h. The mixture was dried completely, and the PA derivatives were reconstituted in 200 μL of ethyl acetate and analyzed by gas chromatography-mass spectrometry (7890A GC/5975C MSD; Agilent).

NO Measurement

NO accumulation was monitored using the NO-sensitive dye DAF-2DA (Sigma-Aldrich) as described previously (Asai et al., 2008). For NO detection, leaves were infiltrated with 200 mM sodium phosphate buffer (pH 7.4) supplemented with 12.5 μM DAF-2DA and then incubated for 1 h in the dark at room temperature. As a positive control, SNP (500 μM) was infiltrated into leaves with DAF-2DA. The fluorescent products of the reaction between DAF-

2DA and NO were observed using a confocal laser scanning microscope with excitation at 470 nm. Emission images at 525 nm were captured using a constant acquisition time, and fluorescence intensity was determined via color histogram analysis.

H_2O_2 Measurement

H_2O_2 accumulation in leaves was quantified using the xylenol orange method (Gay et al., 1999; Choi and Hwang, 2011). Xylenol orange assay reagent was freshly prepared by adding 500 μL of reagent [25 mM $FeSO_4$ and 25 mM $(NH_4)_2SO_4$ in 2.5 M H_2SO_4] to 50 mL of 125 μM xylenol orange in 100 mM sorbitol. Eight leaf discs (0.5 cm^2) were floated on 1 mL of distilled water in a microtube for 1 h, centrifuged for 1 min at 12,000*g*, and 100 μL of supernatant was immediately added to 1 mL of xylenol orange assay reagent. The mixture was incubated for 30 min at room temperature. A standard curve for H_2O_2 was generated from measurements obtained from a serial dilution of 100 nmol to 100 μmol of H_2O_2. H_2O_2 was quantified by measuring the A_{560} using a DU 650 spectrophotometer (Beckman).

Amino Acid Analysis

Amino acids were extracted from pepper leaves with 3% (v/v) 5-SA in 70% (v/v) ethanol as described previously (Hwang et al., 2011). Briefly, leaf extracts were centrifuged at 13,000*g* for 15 min. The pellet was reextracted, and supernatants were pooled. Detection and quantification of amino acids were performed using the PICO-Tag system (Waters; http://www.waters.com). Free amino acids were separated on a Nova-Pak C18 column (4 μm, 3.9 × 3,300 mm; Waters) at 46°C. The sample was injected and eluted with a linear gradient of 0% to 100% (v/v) acetonitrile. Fluorescence was monitored using an HP 1100 Series (Agilent; http://www.chem.agilent.com/) at 254 nm. L-nor-Leu (Sigma-Aldrich; http://www.sigmaaldrich.com/), an amino acid that is not commonly found in proteins, was used as an internal standard.

Sequence data from this article can be found in the GenBank/EMBL data libraries under the following accession numbers: *Xcv avrBsT* (GQ266402), pepper *CaADC1* (KC160547), pepper *CaPR1* (AF053343), pepper *CaPR10* (AF244121), pepper *CaDEF1* (AF442388), tobacco *ADC* (AAQ14851), pea (*Pisum sativum*) *ADC* (CAA85773), Arabidopsis *ADC1* (NP_179243), and Arabidopsis *ADC2* (NP_195197).

Supplemental Data

The following materials are available in the online version of this article.

Supplemental Figure S1. Nucleotide and deduced amino acid sequences of *CaADC1* cDNA.

Supplemental Figure S2. Alignment of CaADC1 with other ADCs.

Supplemental Figure S3. RNA gel-blot analyses of *CaADC1* expression in pepper plants.

Supplemental Figure S4. Coexpression of *CaADC1* does not promote *BAX*-triggered cell death in *N. benthamiana* leaves.

Supplemental Figure S5. CaADC1 forms a complex with the AvrBsT C222A mutant but does not trigger cell death-inducing activity in AvrBsT C222A.

Supplemental Figure S6. Effects of transient expression of *CaADC1* and *AvrBsT* on amino acid levels in *N. benthamiana*.

Supplemental Figure S7. Disease symptoms in empty vector control (TRV:00) and *CaADC1*-silenced (TRV:*CaADC1*) leaves infiltrated with *Xcv* Ds1 (EV) and Ds1 (*avrBsT*).

Supplemental Figure S8. Effects of *CaADC1* silencing on amino acid levels of pepper leaves infected with *Xcv*.

Supplemental Figure S9. GABA and Ala do not inhibit *Xcv* growth in yeast nutrient media.

Supplemental Figure S10. Working model for the role of CaADC1 in signaling mediated by PAs and GABA in cell death and defense responses in plants.

Supplemental Table S1. Gene-specific primers for quantitative RT-PCR analyses.

Supplemental Table S2. Primers for the generation of gene constructs.

Received March 4, 2013; accepted June 18, 2013; published June 19, 2013.

LITERATURE CITED

Alcázar R, García-Martínez JL, Cuevas JC, Tiburcio AF, Altabella T (2005) Overexpression of ADC2 in *Arabidopsis* induces dwarfism and late-flowering through GA deficiency. Plant J **43:** 425–436

Asai S, Ohta K, Yoshioka H (2008) MAPK signaling regulates nitric oxide and NADPH oxidase-dependent oxidative bursts in *Nicotiana benthamiana*. Plant Cell **20:** 1390–1406

Asai T, Tena G, Plotnikova J, Willmann MR, Chiu WL, Gomez-Gomez L, Boller T, Ausubel FM, Sheen J (2002) MAP kinase signalling cascade in *Arabidopsis* innate immunity. Nature **415:** 977–983

Averill-Bates DA, Ke Q, Tanel A, Roy J, Fortier G, Agostinelli E (2008) Mechanism of cell death induced by spermine and amine oxidase in mouse melanoma cells. Int J Oncol **32:** 79–88

Bagni N, Tassoni A (2001) Biosynthesis, oxidation and conjugation of aliphatic polyamines in higher plants. Amino Acids **20:** 301–317

Berger S, Sinha AK, Roitsch T (2007) Plant physiology meets phytopathology: plant primary metabolism and plant-pathogen interactions. J Exp Bot **58:** 4019–4026

Besson-Bard A, Pugin A, Wendehenne D (2008) New insights into nitric oxide signaling in plants. Annu Rev Plant Biol **59:** 21–39

Bhat R, Axtell R, Mitra A, Miranda M, Lock C, Tsien RW, Steinman L (2010) Inhibitory role for GABA in autoimmune inflammation. Proc Natl Acad Sci USA **107:** 2580–2585

Bouché N, Fait A, Bouchez D, Møller SG, Fromm H (2003) Mitochondrial succinic-semialdehyde dehydrogenase of the gamma-aminobutyrate shunt is required to restrict levels of reactive oxygen intermediates in plants. Proc Natl Acad Sci USA **100:** 6843–6848

Bouché N, Fromm H (2004) GABA in plants: just a metabolite? Trends Plant Sci **9:** 110–115

Bouchereau A, Aziz A, Larher F, Martin-Tanguy J (1999) Polyamines and environmental challenges: recent development. Plant Sci **140:** 103–125

Capell T, Bassie L, Christou P (2004) Modulation of the polyamine biosynthetic pathway in transgenic rice confers tolerance to drought stress. Proc Natl Acad Sci USA **101:** 9909–9914

Chen GG, Turecki G, Mamer OA (2009) A quantitative GC-MS method for three major polyamines in postmortem brain cortex. J Mass Spectrom **44:** 1203–1210

Chevrot R, Rosen R, Haudecoeur E, Cirou A, Shelp BJ, Ron E, Faure D (2006) GABA controls the level of quorum-sensing signal in *Agrobacterium tumefaciens*. Proc Natl Acad Sci USA **103:** 7460–7464

Choi HW, Kim YJ, Lee SC, Hong JK, Hwang BK (2007) Hydrogen peroxide generation by the pepper extracellular peroxidase CaPO2 activates local and systemic cell death and defense response to bacterial pathogens. Plant Physiol **145:** 890–904

Choi S, Hwang BK (2011) Proteomics and functional analyses of pepper *abscisic acid-responsive 1* (*ABR1*), which is involved in cell death and defense signaling. Plant Cell **23:** 823–842

Choi S, Hwang IS, Hwang BK (2012) Requirement of the cytosolic interaction between PATHOGENESIS-RELATED PROTEIN10 and LEUCINE-RICH REPEAT PROTEIN1 for cell death and defense signaling in pepper. Plant Cell **24:** 1675–1690

Choi YH, Tapias EC, Kim HK, Lefeber AWM, Erkelens C, Verhoeven JTJ, Brzin J, Zel J, Verpoorte R (2004) Metabolic discrimination of *Catharanthus roseus* leaves infected by phytoplasma using ^{1}H-NMR spectroscopy and multivariate data analysis. Plant Physiol **135:** 2398–2410

Cohen E, Arad SM, Heimer YM, Mizrahi Y (1983) Polyamine biosynthetic enzymes in *Chlorella*: characterization of ornithine and arginine decarboxylase. Plant Cell Physiol **24:** 1003–1010

Cowley T, Walters DR (2002) Polyamine metabolism in barley reacting hypersensitively to the powdery mildew fungus *Blumeria graminis* f.sp *hordei*. Plant Cell Environ **25:** 461–468

Cunnac S, Wilson A, Nuwer J, Kirik A, Baranage G, Mudgett MB (2007) A conserved carboxylesterase is a SUPPRESSOR OF AVRBST-ELICITED RESISTANCE in *Arabidopsis*. Plant Cell **19:** 688–705

Deeb F, van der Weele CM, Wolniak SM (2010) Spermidine is a morphogenetic determinant for cell fate specification in the male gametophyte of the water fern *Marsilea vestita*. Plant Cell **22:** 3678–3691

del Pozo O, Pedley KF, Martin GB (2004) MAPKKKalpha is a positive regulator of cell death associated with both plant immunity and disease. EMBO J **23:** 3072–3082

de Vera N, Martínez E, Sanfeliu C (2008) Spermine induces cell death in cultured human embryonic cerebral cortical neurons through N-methyl-D-aspartate receptor activation. J Neurosci Res **86:** 861–872

Du LQ, Ali GS, Simons KA, Hou JG, Yang TB, Reddy ASN, Poovaiah BW (2009) Ca^{2+}/calmodulin regulates salicylic-acid-mediated plant immunity. Nature **457:** 1154–1158

Durrant WE, Dong X (2004) Systemic acquired resistance. Annu Rev Phytopathol **42:** 185–209

Eitas TK, Dangl JL (2010) NB-LRR proteins: pairs, pieces, perception, partners, and pathways. Curr Opin Plant Biol **13:** 472–477

Escolar L, Van Den Ackerveken G, Pieplow S, Rossier O, Bonas U (2001) Type III secretion and *in planta* recognition of the *Xanthomonas* avirulence proteins AvrBs1 and AvrBsT. Mol Plant Pathol **2:** 287–296

Flores HE, Filner P (1985) Polyamine catabolism in higher plants: characterization of pyrroline dehydrogenase. Plant Growth Regul **3:** 277–291

Garcia-Brugger A, Lamotte O, Vandelle E, Bourque S, Lecourieux D, Poinssot B, Wendehenne D, Pugin A (2006) Early signaling events induced by elicitors of plant defenses. Mol Plant Microbe Interact **19:** 711–724

Gay C, Collins J, Gebicki JM (1999) Hydroperoxide assay with the ferric-xylenol orange complex. Anal Biochem **273:** 149–155

Gonzalez ME, Marco F, Minguet EG, Carrasco-Sorli P, Blázquez MA, Carbonell J, Ruiz OA, Pieckenstain FL (2011) Perturbation of spermine synthase gene expression and transcript profiling provide new insights on the role of the tetraamine spermine in Arabidopsis defense against *Pseudomonas viridiflava*. Plant Physiol **156:** 2266–2277

Hanfrey C, Sommer S, Mayer MJ, Burtin D, Michael AJ (2001) *Arabidopsis* polyamine biosynthesis: absence of ornithine decarboxylase and the mechanism of arginine decarboxylase activity. Plant J **27:** 551–560

Haudecoeur E, Planamente S, Cirou A, Tannieres M, Shelp BJ, Morera S, Faure D (2009) Proline antagonizes GABA-induced quenching of quorum-sensing in *Agrobacterium tumefaciens*. Proc Natl Acad Sci USA **106:** 14587–14592

Hwang IS, An SH, Hwang BK (2011) Pepper asparagine synthetase 1 (CaAS1) is required for plant nitrogen assimilation and defense responses to microbial pathogens. Plant J **67:** 749–762

Ito H, Fukuda Y, Murata K, Kimura A (1983) Transformation of intact yeast cells treated with alkali cations. J Bacteriol **153:** 163–168

Janowitz T, Kneifel H, Piotrowski M (2003) Identification and characterization of plant agmatine iminohydrolase, the last missing link in polyamine biosynthesis of plants. FEBS Lett **544:** 258–261

Kasinathan V, Wingler A (2004) Effect of reduced arginine decarboxylase activity on salt tolerance and on polyamine formation during salt stress in *Arabidopsis thaliana*. Physiol Plant **121:** 101–107

Kim NH (2012) Molecular, immunocytological and metabolic studies of the AvrBsT, AvrBsT-SGT1-PIK1 complex, pepper arginine decarboxylase, heat shock protein 70, aldehyde dehydrogenase and protease inhibitor in plant cell death and defense responses to microbial pathogens. PhD thesis. Korea University, Seoul, Korea

Kim NH, Choi HW, Hwang BK (2010) *Xanthomonas campestris* pv. *vesicatoria* effector AvrBsT induces cell death in pepper, but suppresses defense responses in tomato. Mol Plant Microbe Interact **23:** 1069–1082

Kirik A, Mudgett MB (2009) SOBER1 phospholipase activity suppresses phosphatidic acid accumulation and plant immunity in response to bacterial effector AvrBsT. Proc Natl Acad Sci USA **106:** 20532–20537

Klessig DF, Durner J, Noad R, Navarre DA, Wendehenne D, Kumar D, Zhou JM, Shah J, Zhang S, Kachroo P, et al (2000) Nitric oxide and salicylic acid signaling in plant defense. Proc Natl Acad Sci USA **97:** 8849–8855

Koch E, Slusarenko A (1990) *Arabidopsis* is susceptible to infection by a downy mildew fungus. Plant Cell **2:** 437–445

Kumria R, Rajam MV (2002) Ornithine decarboxylase transgene in tobacco affects polyamines, *in vitro* morphogenesis and response to salt stress. J Plant Physiol **159:** 983–990

Lacomme C, Santa Cruz S (1999) Bax-induced cell death in tobacco is similar to the hypersensitive response. Proc Natl Acad Sci USA **96:** 7956–7961

Lamb C, Dixon RA (1997) The oxidative burst in plant disease resistance. Annu Rev Plant Physiol Plant Mol Biol **48:** 251–275

Lima MRM, Felgueiras ML, Graça G, Rodrigues JEA, Barros A, Gil AM, Dias ACP (2010) NMR metabolomics of esca disease-affected *Vitis vinifera* cv. Alvarinho leaves. J Exp Bot **61:** 4033–4042

Liu Y, Schiff M, Dinesh-Kumar SP (2002) Virus-induced gene silencing in tomato. Plant J **31:** 777–786

Marina M, Maiale SJ, Rossi FR, Romero MF, Rivas EI, Gárriz A, Ruiz OA, Pieckenstain FL (2008) Apoplastic polyamine oxidation plays different roles in local responses of tobacco to infection by the necrotrophic fungus *Sclerotinia sclerotiorum* and the biotrophic bacterium *Pseudomonas viridiflava*. Plant Physiol **147:** 2164–2178

Martin-Tanguy J (2001) Metabolism and function of polyamines in plants: recent development (new approaches). Plant Growth Regul **34:** 135–148

Mitsuya Y, Takahashi Y, Berberich T, Miyazaki A, Matsumura H, Takahashi H, Terauchi R, Kusano T (2009) Spermine signaling plays a significant role in the defense response of *Arabidopsis thaliana* to cucumber mosaic virus. J Plant Physiol **166:** 626–643

Moreau M, Lindermayr C, Durner J, Klessig DF (2010) NO synthesis and signaling in plants: where do we stand? Physiol Plant **138:** 372–383

Moschou PN, Paschalidis KA, Delis ID, Andriopoulou AH, Lagiotis GD, Yakoumakis DI, Roubelakis-Angelakis KA (2008) Spermidine exodus and oxidation in the apoplast induced by abiotic stress is responsible for H_2O_2 signatures that direct tolerance responses in tobacco. Plant Cell **20:** 1708–1724

Orth K, Xu Z, Mudgett MB, Bao ZQ, Palmer LE, Bliska JB, Mangel WF, Staskawicz B, Dixon JE (2000) Disruption of signaling by Yersinia effector YopJ, a ubiquitin-like protein protease. Science **290:** 1594–1597

Park DH, Mirabella R, Bronstein PA, Preston GM, Haring MA, Lim CK, Collmer A, Schuurink RC (2010) Mutations in γ-aminobutyric acid (GABA) transaminase genes in plants or *Pseudomonas syringae* reduce bacterial virulence. Plant J **64:** 318–330

Piotrowski M, Janowitz T, Kneifel H (2003) Plant C-N hydrolases and the identification of a plant N-carbamoylputrescine amidohydrolase involved in polyamine biosynthesis. J Biol Chem **278:** 1708–1712

Roberts MR (2007) Does GABA act as a signal in plants? Plant Signal Behav **2:** 408–409

Rockel P, Strube F, Rockel A, Wildt J, Kaiser WM (2002) Regulation of nitric oxide (NO) production by plant nitrate reductase *in vivo* and *in vitro*. J Exp Bot **53:** 103–110

Rosales EP, Iannone MF, Groppa MD, Benavides MP (2012) Polyamines modulate nitrate reductase activity in wheat leaves: involvement of nitric oxide. Amino Acids **42:** 857–865

Shelp BJ, Bown AW, Faure D (2006) Extracellular gamma-aminobutyrate mediates communication between plants and other organisms. Plant Physiol **142:** 1350–1352

Skopelitis DS, Paranychianakis NV, Paschalidis KA, Pliakonis ED, Delis ID, Yakoumakis DI, Kouvarakis A, Papadakis AK, Stephanou EG, Roubelakis-Angelakis KA (2006) Abiotic stress generates ROS that signal expression of anionic glutamate dehydrogenases to form glutamate for proline synthesis in tobacco and grapevine. Plant Cell **18:** 2767–2781

Szczesny R, Büttner D, Escolar L, Schulze S, Seiferth A, Bonas U (2010) Suppression of the AvrBs1-specific hypersensitive response by the YopJ effector homolog AvrBsT from *Xanthomonas* depends on a SNF1-related kinase. New Phytol **187:** 1058–1074

Takahashi Y, Berberich T, Miyazaki A, Seo S, Ohashi Y, Kusano T (2003) Spermine signalling in tobacco: activation of mitogen-activated protein kinases by spermine is mediated through mitochondrial dysfunction. Plant J **36:** 820–829

Takahashi Y, Uehara Y, Berberich T, Ito A, Saitoh H, Miyazaki A, Terauchi R, Kusano T (2004) A subset of hypersensitive response marker genes, including HSR203J, is the downstream target of a spermine signal transduction pathway in tobacco. Plant J **40:** 586–595

Thordal Christensen H, Zhang Z, Wei Y, Collinge DB (1997) Subcellular localization of H2O2 in plants: H2O2 accumulation in papillae and hypersensitive response during the barley-powdery mildew interaction. Plant J **11:** 1187–1194

Ton J, Mauch-Mani B (2004) β-Amino-butyric acid-induced resistance against necrotrophic pathogens is based on ABA-dependent priming for callose. Plant J **38:** 119–130

Torres MA, Jones JDG, Dangl JL (2006) Reactive oxygen species signaling in response to pathogens. Plant Physiol **141:** 373–378

Tsuda K, Sato M, Stoddard T, Glazebrook J, Katagiri F (2009) Network properties of robust immunity in plants. PLoS Genet **5:** e1000772

Van Breusegem F, Dat JF (2006) Reactive oxygen species in plant cell death. Plant Physiol **141:** 384–390

Walden R, Cordeiro A, Tiburcio AF (1997) Polyamines: small molecules triggering pathways in plant growth and development. Plant Physiol **113:** 1009–1013

Walter M, Chaban C, Schütze K, Batistic O, Weckermann K, Näke C, Blazevic D, Grefen C, Schumacher K, Oecking C, et al (2004) Visualization of protein interactions in living plant cells using bimolecular fluorescence complementation. Plant J **40:** 428–438

Walters DR (2003a) Resistance to plant pathogens: possible roles for free polyamines and polyamine catabolism. New Phytol **159:** 109–115

Walters DR (2003b) Polyamines and plant disease. Phytochemistry **64:** 97–107

Wang PC, Du YY, Li YA, Ren DT, Song CP (2010) Hydrogen peroxide-mediated activation of MAP kinase 6 modulates nitric oxide biosynthesis and signal transduction in *Arabidopsis*. Plant Cell **22:** 2981–2998

Wilms I, Voss B, Hess WR, Leichert LI, Narberhaus F (2011) Small RNA-mediated control of the *Agrobacterium tumefaciens* GABA binding protein. Mol Microbiol **80:** 492–506

Wimalasekera R, Tebartz F, Scherer GF (2011) Polyamines, polyamine oxidases and nitric oxide in development, abiotic and biotic stresses. Plant Sci **181:** 593–603

Yamasaki H, Cohen MF (2006) NO signal at the crossroads: polyamine-induced nitric oxide synthesis in plants? Trends Plant Sci **11:** 522–524

Yun BW, Feechan A, Yin MH, Saidi NBB, Le Bihan T, Yu M, Moore JW, Kang JG, Kwon E, Spoel SH, et al (2011) S-Nitrosylation of NADPH oxidase regulates cell death in plant immunity. Nature **478:** 264–268